Constellation Randomization Achieves Transmit Diversity for Single-RF Spatial Modulation

Christos Masouros, *Senior Member, IEEE*, and Lajos Hanzo, *Fellow, IEEE*

***Abstract*—The performance of spatial modulation (SM) is known to be dominated by the minimum Euclidean distance (MED) in the received SM constellation. In this paper, a symbol-scaling technique is proposed for SM in the multiple-input–multiple-output (MIMO) channel that enhances the MED to improve the performance of SM. This is achieved by forming fixed sets of candidate prescaling factors for the transmit antennas (TAs), which are randomly generated and are known at both the transmitter and the receiver. For a given channel realization, the transmitter chooses the specific set of factors that maximizes the MED. Given the channel state information (CSI) readily available at the receiver for detection, the receiver independently chooses the same set of prescaling factors and uses them for the detection of both the antenna index (AI) and the symbol of interest. We analytically calculate the attainable gains of the proposed technique, in terms of its transmit diversity order, based on both the distribution of the MED and on the theory of classical order statistics. Furthermore, we show that the proposed scheme offers a scalable performance–complexity tradeoff for SM by varying the number of candidate sets of prescaling factors, with significant performance improvements, compared to conventional SM.**

***Index Terms*—Constellation shaping, multiple-input single-output, prescaling, spatial modulation (SM).**

I. Introduction

TRADITIONAL spatial multiplexing has been shown to improve the capacity of the wireless channel by exploiting multiantenna transmitters [1]. More recently, spatial modulation (SM) has been explored as a means of implicitly encoding information in the index of the specific antenna activated for the transmission of the modulated symbols, offering a low-complexity alternative [2]. Its central benefits include the absence of interantenna interference (IAI) and the fact that it only requires a subset (down to one) of radio-frequency (RF) chains compared to spatial multiplexing. Accordingly, the interantenna synchronization is also relaxed. Early work has focused on the design of receiver algorithms for minimizing the bit error rate (BER) of SM at a low complexity [2]–[6]. Matched filtering is shown to be a low-complexity technique for detecting the antenna index (AI) used for SM [2]. A maximum-likelihood (ML) detector is introduced in [4] for reducing the complexity of classic spatial multiplexing ML detectors. Compressive sensing and reduced-space sphere detection have been discussed for SM in [5] and [6] for further complexity reduction.

In addition to receive processing, recent work has also proposed constellation shaping for SM [7]–[15]. Specifically, in [7], the transmit diversity of coded SM is analyzed for different *spatial constellations*, which represent the legitimate sets of activated transmit antennas (TAs). Furthermore, Yang [8] discusses symbol constellation optimization for minimizing the BER. Indeed, spatial- and symbol-constellation shaping are discussed separately, as aforementioned. By contrast, the design of the received SM constellation that combines the choice of the TA, as well as the transmit symbol constellation, is the focus of this paper. Precoding-aided approaches that combine SM with spatial multiplexing are studied in [11] and [12]. A number of constellation-shaping schemes [9]–[15] have also been proposed for the special case of SM, which is referred to as space shift keying, where the information is only carried in the spatial domain, by the activated AI. Their application to the SM transmission, where the transmit waveform is modulated, is nontrivial.

Closely related work has focused on shaping the receive SM constellation by means of symbol prescaling at the transmitter, aiming at maximizing the minimum Euclidean distance (MED) in the received SM constellation [17]–[19]. The constellation-shaping approach in [17] and [18] aims at fitting the receive SM constellation to one of the existing optimal constellation formats in terms of minimum distance, such as, e.g., quadrature amplitude modulation (QAM). Due to the strict constellation fitting requirement imposed on both the amplitude and the phase, this prescaling relies on the inversion of the channel coefficients. In the case of ill-conditioned channels, this substantially increases the power associated to the transmit constellation and therefore requires scaling factors for normalizing the transmit power, which, however, reduces the received signal-to-noise ratio (SNR). This problem has been alleviated in [19], where a constellation-shaping scheme based on phase-only scaling is proposed. Nevertheless, the constellation shaping used in the aforementioned schemes is limited in the sense that it only applies to multiple-input–single-output (MISO) systems where a single symbol is received for each transmission, and thus, the characterization and shaping of the receive SM constellation is simple. The application of constellation shaping in the multiple-input–multiple-output (MIMO) systems is still an open problem.

Manuscript received September 30, 2014; revised June 3, 2015 and November 10, 2015; accepted December 27, 2015. This work was supported by the Royal Academy of Engineering, U.K. The review of this paper was coordinated by Prof. Y. Gong.

C. Masouros is with the Department of Electrical and Electronic Engineering, University College London, London WC1E 7JE, U.K. (e-mail: c.masouros@ucl.ac.uk). AQ1

L. Hanzo is with the School of Electronics and Computer Science, University of Southampton, Southampton SO17 1BJ, U.K. (e-mail: lh@ecs.soton.ac.uk).

Color versions of one or more of the figures in this paper are available online at http://ieeexplore.ieee.org.

Digital Object Identifier 10.1109/TVT.2015.2513380

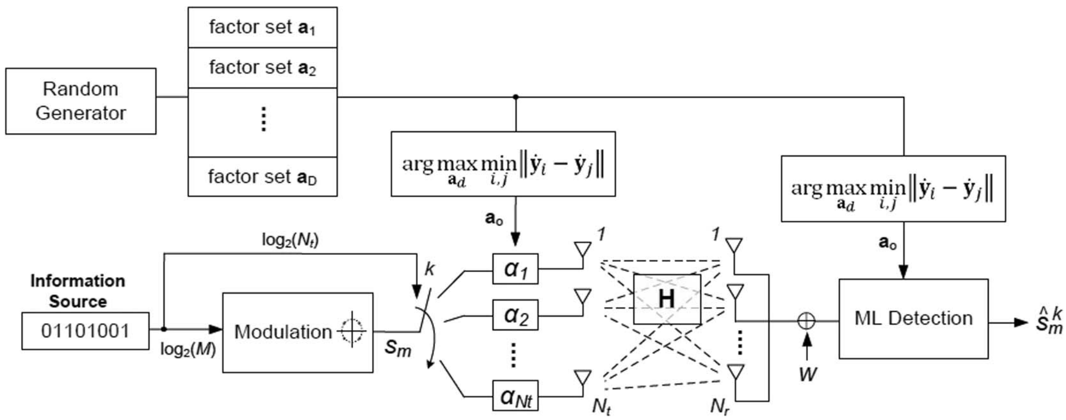

Fig. 1. Block diagram of SM transceiver with constellation randomization (SM-CR).

In line with the aforementioned challenges, in this paper, we introduce a new transmit prescaling (TPS) scheme, where the received constellation fitting problem is relaxed. As opposed to the aforementioned strict constellation fitting approaches, here, the received SM constellation is randomized by TPS for maximizing the MED between its points for a given channel. In more detail, a number of randomly generated candidate sets of TPS factors are formed offline, which are known to both the transmitter and the receiver. Each of these sets is normalized, so that the average transmit power remains unchanged, and yields a different receive constellation for a certain channel realization. For a given channel, the transmitter then selects that particular set of TPS factors that yields the SM constellation having the maximum MED. By doing so, the TPS alleviates the cases where different TAs yield similar received symbols and thus improves the reliability of symbol detection. At the receiver, by exploiting the channel state information (CSI) readily available for detection, the detector selects the same set of TPS factors to form the received constellation and applies an ML test to estimate the data. The explicit benefit of the aforementioned methodology is that it extends the idea of receive SM constellation shaping to the MIMO scenarios having multiple antennas at the receiver, and it will be shown that it introduces additional transmit diversity gains and improves the power efficiency of the SM system. Against this background, we list the main contributions of this paper as follows.

- We propose a new per-antenna TPS scheme for SM-aided point-to-point MIMO transmission that improves the attainable performance.
- We analytically derive a tight upper bound of the transmit diversity gains obtained by the proposed technique, based on the distribution of the MED in the received constellation for transmission over a frequency-flat Rayleigh distributed channel.
- We analyze the computational complexity of the proposed scheme to demonstrate how a scalable performance–complexity tradeoff can be provided by the proposed technique, when adapting the number of candidate sets of TPS factors.
- Using the aforementioned performance and complexity analyses, we study the power efficiency of the proposed scheme in comparison to conventional SM. We introduce a power efficiency metric that combines the transmit power, the achieved throughput, and the computational complexity imposed to quantify the improved power efficiency offered by the proposed scheme.

The remainder of this paper is organized as follows. Section II presents the MIMO system model and introduces the SM transmission. Section III details the proposed TPS scheme, while in Section IV, we present our analytical study of the obtained transmit diversity gains of the proposed scheme. Sections V and VI detail the complexity calculation and the study of the attainable power efficiency. Section VII presents our numerical results, and finally, our conclusions are offered in Section VIII.

II. System Model and Spatial Modulation

A. System Model

Consider a MIMO system where the transmitter and receiver are equipped with N_t and N_r antennas, respectively. For simplicity, unless stated otherwise, in this paper, we assume that the transmit power budget is limited to unity, i.e., $P = 1$. See [20]–[22] for extensive reviews and tutorials on the basics and state-of-the-art on SM. Here, we focus on the single-RF-chain SM approach, where the transmit vector is in the all-but-one zero form $\mathbf{s}_m^k = [0, \ldots, s_m, \ldots, 0]^T$, where the notation $[.]^T$ denotes the transpose operator. Here, $s_m, m \in \{1, \ldots, M\}$ is a symbol taken from an M-order modulation alphabet that represents the transmitted waveform in the baseband domain conveying $\log_2(M)$ bits, and k represents the index of the activated TA (the index of the nonzero element in $\mathbf{s}_m^k$) conveying $\log_2(N_t)$ bits in the spatial domain. Clearly, since $\mathbf{s}$ is an all-zero vector apart from s_m^k, there is no IAI.

The per-antenna TPS approach, which is the focus of this paper, is shown in Fig. 1. The signal fed to each TA is scaled by a complex-valued coefficient $\alpha_k, k \in \{1, \ldots, N_t\}$, for which we have $E\{|\alpha_k|\} = 1$, where $|x|$ denotes the amplitude of a complex number x, and $E\{.\}$ denotes the expectation operator. Defining the MIMO channel vector as $\mathbf{H}$, with elements $h_{i,j}$ representing the complex channel coefficient between the ith TA to the jth receive antenna (RA), the received symbol vector can be written as

$$\mathbf{y} = \mathbf{H}\mathbf{A}\mathbf{s}_m^k + \mathbf{w} \tag{1}$$

where $\mathbf{w} \sim \mathcal{CN}(0, \sigma^2 \mathbf{I})$ is the additive white Gaussian noise component at the receiver, with $\mathcal{CN}(\mu, \sigma^2)$ denoting the circularly symmetric complex Gaussian distribution with mean μ and variance σ^2. Furthermore, $\mathbf{A} = \mathrm{diag}(\mathbf{a}) \in \mathbb{C}^{N_t \times N_t}$ is the TPS matrix with $\mathbf{a} = [\alpha_1, \alpha_2, \ldots, \alpha_{N_t}]$, and $\mathrm{diag}(\mathbf{x})$ represents the diagonal matrix with its diagonal elements taken from vector $\mathbf{x}$. Note that the diagonal structure of $\mathbf{A}$ guarantees having a transmit vector $\mathbf{t} = \mathbf{A}\mathbf{s}$ with a single nonzero element, so that the single-RF-chain aspect of SM is preserved.

At the receiver, a joint ML detection of both the TA index and the transmit symbol is obtained by the minimization

$$\begin{aligned}[\hat{s}_m, \hat{k}] &= \arg\min_i \|\mathbf{y} - \mathbf{y}_i\| \\ &= \arg\min_{m,k} \left\|\mathbf{y} - \mathbf{H}\mathbf{A}\mathbf{s}_m^k\right\| \end{aligned} \tag{2}$$

where $\|\mathbf{x}\|$ denotes the norm of vector $\mathbf{x}$, and $\mathbf{y}_i$ is the ith constellation point in the received SM constellation. By exploiting the specific structure of the transmit vector, this can be further simplified to

$$[\hat{s}_m, \hat{k}] = \arg\min_{m,k} \left\|\mathbf{y} - \mathbf{h}_k \alpha_m^k s_m\right\| \tag{3}$$

where $\mathbf{h}_k$ denotes the kth column of matrix $\mathbf{H}$, and α_m^k is the TPS coefficient of the kth TA. It is widely recognized that the performance of the detection, as explained earlier, is dominated by the MED between adjacent constellation points $\dot{\mathbf{y}}_i, \dot{\mathbf{y}}_j$ in the receive SM constellation, i.e.,

$$d_{\min} = \min_{i,j} \|\mathbf{y}_i - \mathbf{y}_j\|^2, i \neq j. \tag{4}$$

Accordingly, to improve the likelihood of correct detection, constellation-shaping TPS schemes for SM aim at maximizing this MED. The optimum TPS matrix $\mathbf{A}^*$ can be found by solving the optimization

$$\begin{aligned}\mathbf{A}^* &= \arg\max_{\mathbf{A}} \min_{i,j} \|\mathbf{y}_i - \mathbf{y}_j\|^2, i \neq j \\ \text{s.t.c.} \quad & \mathrm{trace}(\mathbf{A}^{*H}\mathbf{A}^*) \leq P \end{aligned} \tag{5}$$

and, additionally for single-RF-chain SM, subject to $\mathbf{A}^*$ having a diagonal structure. As aforementioned, $\mathbf{A}^H$ and $\mathrm{trace}(\mathbf{A})$ represent the Hermitian transpose and trace of matrix $\mathbf{A}$, respectively. The aforementioned optimization, however, is an NP-hard problem, which makes finding the TPS factors prohibitively complex and motivates the conception of lower complexity suboptimal techniques.

B. *Prescaling for the MISO Channel*

In line with the aforementioned discussions, in [17], a prescaling scheme is proposed for the MISO channel. Assuming a channel vector $\mathbf{h}$, the receive SM constellation is fitted to a Q-QAM constellation with $Q = N_t M$ by choosing

$$\tilde{\alpha}_m^k = \frac{q_{(m-1)M+k}\|\mathbf{h}\|}{h_k s_m \sqrt{N_t}} \tag{6}$$

where q_i is the ith constellation point in the Q-QAM constellation, and the factor $\|\mathbf{h}\|/\sqrt{N_t}$ is used for normalizing the receive constellation so that $E\{|q|\} = 1$.

We note that, while the scaling in (6) normalizes the receive constellation, it does not normalize the transmit power. Therefore, power-normalized scaling coefficients should be used in the form

$$\alpha_m^k = \frac{\tilde{\alpha}_m^k}{\|\tilde{\mathbf{a}}\|}. \tag{7}$$

Nevertheless, it can be seen that for ill-conditioned channel coefficients, even for just one of the TAs, this leads to low power-scaling factors $f = 1/\|\tilde{\mathbf{a}}\|$, which limits the obtainable performance. Finally, note that α_m^k are data dependent for this approach, as evidenced by the index m, which does not allow for a fixed per-antenna scaling coefficient, as shown in Fig. 1. Most importantly, the aforementioned strict constellation fitting cannot be extended to systems having multiple RAs, since the inversion of the full channel matrix $\mathbf{H}$ would result in nonzero elements in the transmit vector $\mathbf{t}$, which means that all TAs are used. Therefore, the important benefit of single-RF transmission of SM is lost.

An alternative is shown in [19], again for the MISO channel, where the scaling factors are in the form

$$\alpha_k = e^{j\varphi_k} \tag{8}$$

$$\varphi_k = \theta_i - \vartheta_k \tag{9}$$

where ϑ_k is the phase of the kth channel, and θ_i is the ith angle taken from an equally spaced angle arrangement within $[0, 2\pi)$ in the form

$$\theta_i = \frac{2\pi}{N_t M}(i-1), i \in \{1, \ldots, N_t\}. \tag{10}$$

In this way, the phases of the points in the receive SM constellation become equispaced, hence maintaining a minimum for the Euclidean distances in the constellation.

Aside from their individual limitations and the fact that they are suboptimal, the aforementioned prescaling methods are limited by the fact that they apply solely to MISO systems relying on a single RA and cannot be readily extended to the case of MIMO SM transmission, hence lacking receive diversity.

III. Proposed Constellation Randomization Prescaling (SM-CR)

To alleviate the drawbacks of the aforementioned techniques, we propose an adaptive TPS technique that randomizes the received SM constellation. The proposed constellation randomization (CR) simply selects the "best" from a number of randomly generated sets of per-antenna TPS factors, with the aim of improving the resulting MED. By allowing the randomization of the amplitude and phase of the effective channel that combines the TPS factor and the channel gains of the TA, the proposed scheme relaxes the constellation optimization problem and facilitates a better solution for the maximization of $d_{\min}$. In addition, through the aforementioned randomization and selection of the appropriate TPS factors, the proposed scheme critically improves the transmit diversity of the SM system, as will be shown analytically in the following section. The proposed scheme involves the steps as analyzed in the following.

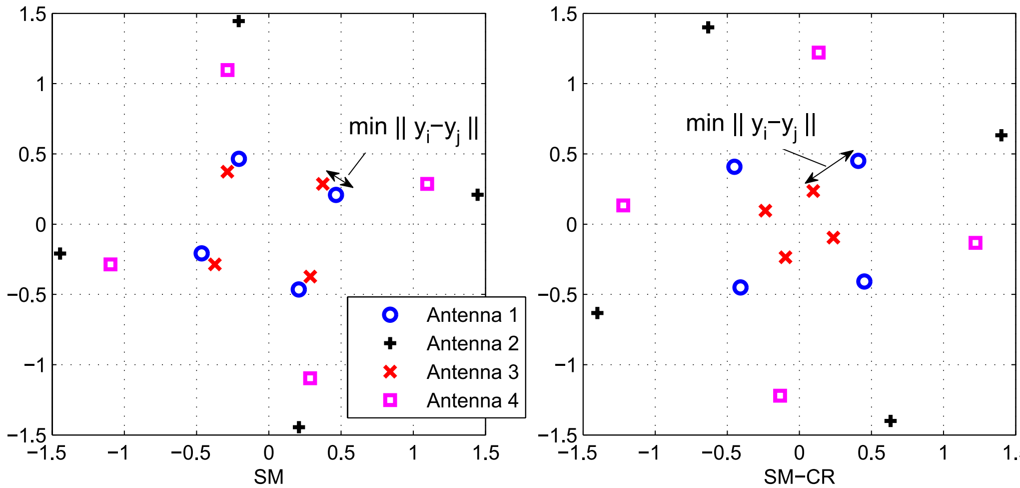

Fig. 2. Received constellation for a 4×1 MISO with SM and SM-CR for 4QAM.

A. *Formation of Candidate Prescaling Sets*

First, a number of D candidate TPS vectors are generated randomly in the form $\mathbf{a}_d$, where $d \in [1, D]$ denotes the index of the candidate set, and $\mathbf{a}_d$ is formed by the elements $\alpha_m^{k(d)} \sim \mathcal{CN}(0, 1)$. These are made available to both the transmitter and the receiver once, in an offline fashion before transmission. These assist in randomizing the received constellation, which is most useful in the cases where two points in the constellation of $\mathbf{Hs}_m^k, m \in [1, M], k \in [1, N_t]$ happen to be very close. To ensure that the average transmit power remains unchanged, the scaling factors are normalized as in (7). It is important to reiterate that, in this work, we focus on power-normalized scaling factors, and hence, the proposed scheme does not constitute a power-allocation scheme. This allows us to isolate the diversity gains from the power and coding gains in our analysis in the following section. In the generalized case, power allocation could be applied on top of the prescaling, by employing a diagonal power-allocation matrix, while the resulting diversity gains would not change.

B. *Selection of Prescaling Vector*

For a given channel, based on the knowledge of vectors $\mathbf{a}_d$, both the transmitter and the receiver can determine the received SM constellation for every d by calculating the set of $[m, k]$ possibilities in

$$\hat{\mathbf{y}} = \mathbf{HA}_d \mathbf{s}_m^k \tag{11}$$

where $\mathbf{A}_d = \mathrm{diag}(\mathbf{a}_d)$ is the diagonal matrix that corresponds to the candidate set $\mathbf{a}_d$. Then, for the given channel coefficients, the transmitter and receiver can independently choose the scaling vector $\mathbf{a}_o$, for which

$$\mathbf{a}_o = \arg\max_d \min_{\substack{m_1,m_2,k_1,k_2 \\ \{m_1,k_1\} \neq \{m_2,k_2\}}} \left\| \mathbf{HA}_d \mathbf{s}_{m_1}^{k_1} - \mathbf{HA}_d \mathbf{s}_{m_2}^{k_2} \right\|^2 . \tag{12}$$

The transmitter then sends $\mathbf{t} = \mathbf{A}_o \mathbf{s}_m^k$, with $\mathbf{A}_o = \mathrm{diag}(\mathbf{a}_o)$, and the receiver applies the ML detector according to

$$[\hat{s}_m, \hat{k}] = \arg\min_{m,k} \|\mathbf{y} - \mathbf{HA}_o \mathbf{s}_m^k\|. \tag{13}$$

As mentioned earlier, since the channel coefficients are estimated at the receiver for detection [2]–[6], (12) can be used to derive the aforementioned factors independently at the receiver. Therefore, no feed forwarding of $\alpha_m^{k(d)}$ or the index d is required. Indeed, for equal channel coefficients available at the transmitter and receiver, they both select the same TPS vector $\mathbf{a}_o$ independently, as per (12). Alternatively, to dispose of the need for CSI at the transmitter (CSIT), the receiver can indeed select the best scaling factors using (12) and feed the index of the selected scaling vector $\mathbf{a}_o$ out of the D candidates back to the transmitter, using $\lceil \log_2 D \rceil$ bits. In comparison to the closely related works in [17]–[19], this provides the proposed scheme with the advantage of a reduced transmit complexity that, instead of CSIT acquisition and prescaling optimization, involves the detection of $\lceil \log_2 D \rceil$ bits at the end of every channel coherence period, and a single complex multiplication of the classically modulated symbol s_m with the prescaling factor a_m^k in the form shown in (3).

The intuitive benefits of the proposed scheme in the MED of the received SM constellation are shown in Fig. 2 for a (4×1)-element MISO system employing 4QAM modulation at high SNR, where the original receive SM constellation without TPS is shown in the left-hand side, and the constellation after the selection in (12) is illustrated on the right-hand side. A clear increase in the MED can be observed, without increasing the average transmit power. In fact, for the example in Fig. 2, a slight reduction of the power in the symbols denoted by "$\times$" can be observed, which, nevertheless, increases the MED in the constellation.

Observe in Fig. 2 that while suboptimal in the constellation design sense, the proposed TPS enhances the MED in the constellation with respect to conventional SM, while imposing a conveniently scalable complexity as per the size of candidate sets D. It is evident that the gains in the MED for the proposed scheme are dependent on the set size D of the candidate TSP vector sets $\mathbf{a}_d$ to choose from. An indicative result of this dependence is shown in Fig. 3, where the average gains in the MED are shown, with increasing numbers of D for different transmission scenarios. Theoretically derived upper bounds for these gains for $N_r = 1$, $N_r = 2$, and $N_r = 4$, based

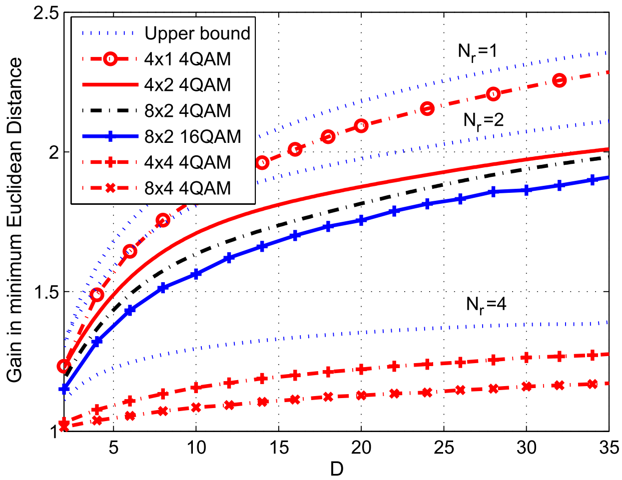

Fig. 3. Gain G in average MED for SM-CR with respect to SM for increasing D.

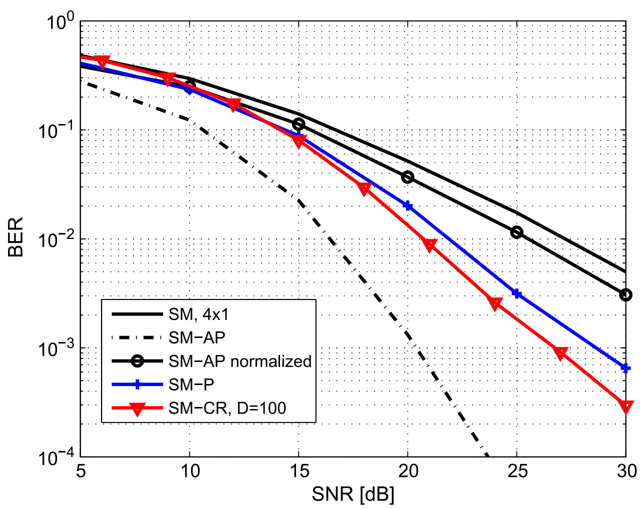

Fig. 4. BER versus SNR for a (4×1) MISO with SM, SM-AP [17], SM-P [19], and SM-CR with $D = 100$ for 4QAM.

on Theorem 1 of the following section, are also shown in the figure and will be detailed in the following. It can be seen that, for low values of D, significant MED benefits are obtained by increasing the number of candidates, while the gains saturate in the region of higher values of D. This justifies the choice of low values of D to constrain the computational complexity involved in the search in (12). In the results that follow, we explore the error rates and complexity and their tradeoff in terms of power efficiency as a means of optimizing the value of D for different performance targets.

IV. Diversity Analysis

A. Transmit Diversity

The proposed CR scheme leads to an increase in the transmit diversity gains. That is, while the transmit diversity of the single-RF SM is known to be one [7], the proposed TPS introduces an amplitude–phase diversity in the transmission, due to the existence of D candidate sets of TPS factors from which to choose. The system is said to have a diversity order of δ, if the BER decays with $\gamma^{-\delta}$ in the high-SNR region, with γ being the SNR (see Fig. 4). To analyze the attainable diversity order, we note the pairwise error probability (PEP) for SM scales with the Euclidean distance between constellation points as [7]

$$\text{PEP}\,(\mathbf{y}_i, \mathbf{y}_j) = \mathcal{Q}\left(\sqrt{\frac{\|\mathbf{y}_i - \mathbf{y}_j\|^2}{2\sigma^2}}\right) \tag{14}$$

where $\mathcal{Q}(x)$ denotes the Gaussian Q-function [25], and

$$\begin{aligned}\|\mathbf{y}_i - \mathbf{y}_j\| &= \sqrt{\|\mathbf{y}_i\|^2 + \|\mathbf{y}_j\|^2 - 2\mathbf{y}_i \bullet \mathbf{y}_j}\\ &= \sqrt{\|\mathbf{y}_i\|^2 + \|\mathbf{y}_j\|^2 - 2\|\mathbf{y}_i\|\|\mathbf{y}_j\|\cos(\Delta\phi)}\end{aligned} \tag{15}$$

where $\mathbf{a} \bullet \mathbf{b}$ denotes the dot product of vectors, and $\Delta\phi$ denotes the phase difference between the two constellation points. Accordingly, for the purposes of characterizing the diversity order, we define the gain in the MED for the proposed SM-CR as

$$\begin{aligned}G(D) &\hat{=} \frac{E\{\max_d d_{\min}^d\}}{E\{d_{\min}\}}\\ &= \frac{E\{\max_d \min_{m,k} \|\mathbf{H}\mathbf{A}_d\mathbf{s}_{m_1}^{k_1} - \mathbf{H}\mathbf{A}_d\mathbf{s}_{m_2}^{k_2}\|^2\}}{E\{\min_{m,k} \|\mathbf{H}\mathbf{s}_{m_1}^{k_1} - \mathbf{H}\mathbf{s}_{m_2}^{k_2}\|^2\}}\end{aligned} \tag{16}$$

where we have used the notation $G(D)$ to suggest that the gain is a function of the size of candidate sets D. It will be shown in the results section that this gain also represents the transmit diversity gain attained. The following theorem describes an upper bound of this diversity gain.

Theorem 1: For a frequency-flat Rayleigh fading channel $\mathbf{H} \sim \mathcal{CN}(0, (1/2)\mathbf{I}_{N_r} \oplus \mathbf{I}_{N_t})$, the gain in the MED of the proposed SM-CR is upper bounded as

$$G(D) \leq G_u = \sum_{k=1}^{D} \binom{D}{k} (-1)^{k+1} e^{n(k-1)} \frac{Ei(-nk, nk)}{Ei(-n, n)} \tag{17}$$

where $n \hat{=} \binom{N_t M}{2}$, with $\binom{p}{q} = p!/q!(p-q)!$ denoting the binomial coefficient, with $x!$ being the factorial function and $Ei(-n, n)$ denoting the generalized exponential integral function [25].

Proof: To simplify the analysis, we shall assume that the distances in the receive constellation are statistically independent. It is shown in Fig. 2 that, strictly speaking, this is not true since the constellation points created by each channel are indeed interdependent through the transmit symbol constellation. Nevertheless, we will demonstrate in Fig. 3 that this affordable assumption yields a tight upper bound for the gain. First, regarding the product $\mathbf{H}\mathbf{A}_d$, it has been shown in [26] that the product of uncorrelated zero-mean Gaussian variables with variances σ_1^2, σ_2^2 is also zero-mean Gaussian with a variance equal to $\sigma_\Pi^2 = \sigma_1^2\sigma_2^2$. It is therefore clear that, for a normalized transmit constellation, the receive vectors are distributed as $\mathbf{y}_i \sim \mathcal{CN}(0, 1/2\mathbf{I}_{N_r})$. Accordingly, $\mathbf{y}_i - \mathbf{y}_j \sim \mathcal{CN}(0, \mathbf{I}_{N_r})$, and therefore, $z \hat{=} \|\mathbf{y}_i - \mathbf{y}_j\|^2 \sim \mathcal{X}_{2N_r}^2$, where $\mathcal{X}_k^2$ denotes the chi-square distribution with k degrees of freedom [25]. The probability density function (PDF) and cumulative distribution function (CDF) of z are, therefore, given by

$$f_z(x) = \frac{1}{2^{N_r}\Gamma(N_r)} x^{N_r - 1} e^{-x/2} \tag{18}$$

$$F_z(x) = \frac{1}{\Gamma(N_r)} \gamma\left(N_r, \frac{x}{2}\right) \tag{19}$$

where $\Gamma(.)$ and $\gamma(.,.)$ denote the Gamma and lower incomplete Gamma functions, respectively [25]. Based on the theory of order statistics [27], from the $n \hat{=} \binom{N_t M}{2}$ distances in the receive SM constellation (see Fig. 2), the minimum distance is distributed as

$$\begin{aligned} f_{d_{\min}}(x) &= n f_z(x)[1 - F_z(x)]^{n-1} \\ &= \frac{n}{2^{N_r}\Gamma(N_r)^n} x^{N_r-1} e^{-x/2} \left[\Gamma\left(N_r, \frac{x}{2}\right)\right]^{n-1} \quad (20) \\ F_{d_{\min}}(x) &= 1 - (1 - F_z(x))^n \\ &= 1 - \left[\frac{1}{\Gamma(N_r)}\Gamma\left(N_r, \frac{x}{2}\right)\right]^n \quad (21) \end{aligned}$$

where $\Gamma(.,.)$ denotes the upper incomplete Gamma function and, as mentioned earlier, it is assumed that all distances in the receive SM constellation are independent. Since $d_{\min}$ is nonnegative, its mean is found as

$$\begin{aligned} E\{d_{\min}\} &= \int_0^\infty [1 - F_{d_{\min}}(x)]dx \\ &= \int_0^\infty [1 - F_z(x)]^n dx. \end{aligned} \quad (22)$$

Let us now derive the mean of the maximum minimum distance in the receive SM constellation as per the proposed technique. We note that, for the normalized TPS factors in (7), the distribution of $\mathbf{y}_i$ remains unchanged. Therefore, the PDF and CDF of $\tau \hat{=} \max_{\mathbf{A}_d} d_{\min}$, when selecting the maximum from D, candidates are given as

$$f_\tau(x) = D f_{d_{\min}}(x) F_{d_{\min}}(x)^{D-1} \quad (23)$$

$$F_\tau(x) = F_{d_{\min}}(x)^D. \quad (24)$$

Similarly to the aforementioned calculation, for the mean of $\tau \hat{=} \max_{\mathbf{A}_d} d_{\min}$, we have

$$\begin{aligned} E\{\tau\} &= \int_0^\infty \{1 - F_\tau(x)\}\, dx \\ &= \int_0^\infty \left\{1 - F_{d_{\min}}(x)^D\right\} dx \\ &= \int_0^\infty \left\{1 - [1 - (1 - F_z(x))^n]^D\right\} dx \\ &= \int_0^\infty \left\{1 - \sum_{k=0}^{D} \binom{D}{k} (-1)^k (1 - F_z(x))^{nk}\right\} dx \\ &= \sum_{k=1}^{D} \binom{D}{k} (-1)^{k+1} \int_0^\infty (1 - F_z(x))^{nk} dx. \end{aligned} \quad (25)$$

As stated previously, we have used the binomial expansion $(1-x)^m = \sum_{k=0}^m \binom{m}{k}(-1)^k x^k$. By substituting (22) and (25) into (16), we arrive at the upper bound for the gain in the MED as

$$G_u(N_r) = \sum_{k=1}^{D} \binom{D}{k} (-1)^{k+1} \frac{\int_0^\infty (1 - F_z(x))^{nk} dx}{\int_0^\infty (1 - F_z(x))^n dx} \quad (26)$$

where we have used the notation $G_u(N_r)$ to clarify that the upper bound here is a function of N_r. Finally, it can be shown that $(dG_u(N_r)/dN_r) \leq 0$, and therefore, the gain is a monotonically decreasing function of the number of RAs. Hence, the gain for the case $N_r = 1$ provides a global upper bound for all cases of N_r. Indeed, as it is shown in Fig. 3 and is intuitive, the highest gains can be observed for the single-antenna receiver case, which experiences a diversity of one for conventional SM. For this case, from (18), (19), and (26), we get (17). ■

B. Error Probability Trends

Based on the aforementioned diversity calculations, we can derive the BER performance of the proposed scheme in the high-SNR region. Indeed, SM systems with N_r uncorrelated RAs have been shown to experience a unit transmit diversity order and receive diversity order of N_r. Accordingly, since the proposed scheme attains a transmit diversity order of $G(D)$, the total diversity becomes $\delta = N_r G(D)$. The resulting probability of error P_e follows the trend

$$P_e = \alpha \gamma^{-N_r G(D)} \quad (27)$$

where γ is the transmit SNR, $\delta = N_r G(D)$ is the diversity order based on the calculations of $G(D)$ in Section IV-A, and α is an arbitrary coefficient. The diversity order $\delta = N_r G(D)$ accounts for the inherent receive diversity N_r in the system and the transmit diversity $G(D)$ induced by the proposed scheme. Clearly, as per the upper bound of Theorem 1 in (17) and the P_e trend in (27), a lower bound in the resulting probability of error can be obtained. In the following results, we show that the aforementioned performance trend matches the simulated performance in the high-SNR region.

V. Computational Complexity

It is clear from the aforementioned discussion that the proposed SM-CR leads to an increase in the computational complexity, with respect to conventional SM, due to the need to compute the MED for all the D candidate scaling factor sets. Here, we analyze the increase in computational complexity at the receiver. We later use this analysis to model the power consumption associated with the required signal processing and compare the proposed SM-CR with conventional SM, in terms of the overall power efficiency of transmission. For reference, we have assumed an LTE Type 2 TDD frame structure [28]. This has a 10-ms duration, which consists of 10 subframes, out of which five subframes, containing 14 symbol time slots each, are used for downlink transmission yielding a block size of $B = 70$ for the downlink, while the rest are used for both uplink and control information transmission. A slow-fading channel is assumed, where the channel remains constant for the duration of the frame. In Table I, we summarize the computationally dominant operations involved at the receiver for both SM and SM-CR. In these calculations, we have used the fact that the calculation of the norm of a vector with n elements involves $2n$ elementary operations. In addition, it can be seen that the product $\mathbf{A}_d \mathbf{s}_m^k$ is a scalar that involves a single complex-valued multiplication, and its multiplication with the channel matrix involves an additional $2N_r$ elementary operations per

TABLE I
COMPLEXITY FOR SM AND THE PROPOSED SM-CR SCHEME

SM-CR	Operations	SM	Operations
Constellation Optimization		*Constellation Calculation*	
$\mathbf{HA}_d\mathbf{s}_m^k, \forall m, k$ $\times D$	$(2N_r+1)N_tMD$	$\mathbf{Hs}_m^k, \forall m, k$	$(2N_r+1)N_tM$
$\mathbf{f}_{m_1,m_2}^{k_1,k_2(d)} = \|\|\mathbf{HA}_d\mathbf{s}_{m_1}^{k_1} - \mathbf{HA}_d\mathbf{s}_{m_2}^{k_2}\|\|$, $\forall m_1, m_2, k_1, k_2, m_1 \neq m_2, k_1 \neq k_2$ $\times D$	$2N_r\binom{N_tM}{2}D$		
$d_{min}^{(d)} = \min\{\mathbf{f}_{m_1,m_2}^{k_1,k_2(d)}\}$ $\times D$	$\binom{N_tM}{2}D$		
$\mathbf{A}_o = \arg\max d_{min}^{(d)}$	D		
ML Detection			
$g_m^k = \|\|\mathbf{y} - \mathbf{HA}_o\mathbf{s}_m^k\|\|^2, \forall m, k$ $\times B$	$2N_tMN_rB$	$g_m^k = \|\|\mathbf{y} - \mathbf{Hs}_m^k\|\|^2, \forall m, k$ $\times B$	$2N_tMN_rB$
$\arg\min g_m^k$ $\times B$	N_tMB	$\arg\min g_m^k$ $\times B$	N_tMB
Total: $(2Nr+1)\left[\binom{N_tM}{2} + N_tM\right]D + D + (2N_r+1)N_tMB$		Total: $(2N_r+1)N_tM(B+1)$	

constellation point. This has to be done for each of the N_tM points in the receive constellation. Accordingly, there are a number of $\binom{N_tM}{2}$ distances in the constellation, and therefore, there are $\binom{N_tM}{2}$ norms in the form of (12) that need to be calculated for each candidate scaling factor set. The first three operations in the constellation optimization in Table I need to be done for each candidate set: hence, D times in total. For the ML detection, a number of N_tM norms in the form of (13) need to be calculated before the minimum is chosen, and this has to be calculated B times in the frame. Finally, we have used the fact that finding the maximum and the minimum in an n-element vector requires n operations.

Based on the aforementioned calculations, we have the complexities of the SM receiver and of the SM-CR receiver, respectively, in the form of

$$C_{\mathrm{SM}}(D) = (2N_r+1)N_tM(B+1) \tag{28}$$

$$C_{\mathrm{SM-CR}}(D) = (2Nr+1)\left[\binom{N_tM}{2} + N_tM\right]D + D + (2Nr+1)N_tMB \tag{29}$$

where it can be seen that the complexity of SM-CR is in the form

$$C_{\mathrm{SM-CR}}(D) = \chi D + \psi \tag{30}$$

with

$$\chi = (2Nr+1)\left[\binom{N_tM}{2} + N_tM\right] + 1 \tag{31}$$

$$\psi = (2Nr+1)N_tMB. \tag{32}$$

In the following section, we use these expressions to calculate the resulting power consumption related to signal processing at the receiver for the evaluation of the power efficiency of transmission.

VI. POWER EFFICIENCY

As the ultimate metric for evaluating the performance–complexity tradeoff and the overall usefulness of the proposed technique, and toward an energy-efficient communication system, we consider the power efficiency of SM-CR compared to SM, as well as its dependence on the number of candidate scaling factor sets D. We note that prior studies explore the energy efficiency of SM for the purposes of optimizing the number of antennas employed [30], [31]. Following the modeling in [29] and [32]–[35], we define the transmit power efficiency of the communication link as the bit rate per total transmit power dissipated, i.e., the ratio of the throughput achieved over the consumed power as

$$\mathcal{P} = \frac{T}{P_{\mathrm{PA}} + (1+N_r)\cdot P_{\mathrm{RF}} + p_c \cdot C} \tag{33}$$

where $P_{\mathrm{PA}} = ((\xi/\eta) - 1)P$ in watts is the power consumed at the power amplifier to produce the total transmit signal power P, with η being the power amplifier efficiency and ξ being the modulation-dependent peak-to-average power ratio. Furthermore, $P_{\mathrm{RF}} = P_{\mathrm{mix}} + P_{\mathrm{filt}} + P_{\mathrm{DAC}}$ is the power related to the mixers, to the transmit filters, and to the digital-to-analog converter (DAC), which is assumed constant for the purposes of this work. We use practical values of these from [32] as $\eta = 0.35$ and $P_{\mathrm{mix}} = 30.3$ mW, $P_{\mathrm{filt}} = 2.5$ mW, and $P_{\mathrm{DAC}} = 1.6$ mW, yielding $P_{\mathrm{RF}} = 34.4$ mW. In (33), p_c in watts/Kops is the power per 10^3 elementary operations (KOps) of the digital signal processor (DSP), and C is the number of operations involved. This term is used to introduce complexity as a factor of the transmitter power consumption in the power efficiency AQ3 metric. Typical values of p_c include $p_c = 22.88$ mW/KOps for the Virtex-4 and $p_c = 5.76$ mW/KOps for the Virtex-5 field-programmable gate array family from Xilinx [36]. Finally AQ4

$$T = \mathcal{E}B(1-P_B) = \mathcal{E}B(1-P_e)^B \tag{34}$$

represents the achieved throughput, where P_B is the block error rate, and

$$\mathcal{E} = \log_2(N_tM) \tag{35}$$

is the spectral efficiency of SM in bits per channel use. For a given transmit power and numbers of TAs and RAs, combining (33) with (27), the power efficiency expression for SM-CR takes the form

$$\mathcal{P} = \frac{\mathcal{E}B(1-\alpha\gamma^{-N_rG(D)})^B}{c + p_cC(D)} \tag{36}$$

where both $G(D)$ and $C(D)$ are functions of the number of candidate sets D through (26) and (29), while α, c are constants. This expression can therefore be used to characterize the scalable performance–complexity tradeoff for the proposed scheme and for optimizing the value of D for maximizing power efficiency.

The expression in (33) provides an amalgamated metric that combines throughput, complexity, and transmit signal power, all in a unified metric. By varying the number of candidate scaling factor sets D, both the resulting complexity and transmission rates are influenced, as shown earlier. Therefore, a scalable tradeoff between performance and complexity can be achieved accordingly. High values of $\mathcal{P}$ indicate that high bit rates are achievable for a given power consumption, and thus denote a high energy efficiency. The following results show that SM-CR provides an increased energy efficiency compared to SM in numerous scenarios using different transmit powers P.

VII. Simulation Results

To evaluate the benefits of the proposed technique, this section presents numerical results based on Monte Carlo simulations of conventional SM without scaling (termed as SM in the figures) and the proposed SM-CR. Our focus is on systems where the receiver employs more than one antenna, where the prescaling schemes in [17]–[19] are inapplicable. The channel impulse response is assumed to be perfectly known at the transmitter. Without loss of generality, unless stated otherwise, we assume that the transmit power is restricted to $P = 1$. MIMO systems with up to eight TAs employing 4QAM and 16QAM modulation are explored, albeit it is plausible that the benefits of the proposed technique extend to larger scale systems and higher order modulation.

First, for reasons of reference, the BER performance of the proposed scheme is compared with the performance of the most relevant techniques in [17] and [19] for the MISO channel, where the latter techniques are applicable. First, we note the performance loss when applying power scaling to the scheme in [17]. Second, while the true strength of the proposed lies in the fact that it applies to MIMO links where the schemes in [17] and [19] are inapplicable, the results here show that the proposed scheme outperforms the conventional techniques in the MISO channel as well.

Next, we show the BER performance with increasing transmit SNR for a (4×2)-element MIMO employing 4QAM, for various numbers of candidate scaling factor sets D, in Fig. 5. The graph includes the performance of SM for the (4×4)-element MIMO for reference. It can be seen that the slope of the BER curves increases with increasing D, which indicates an increase in transmit diversity order. Indeed, for high values of D, the (4×2)-element system with SM-CR exhibits the same transmit diversity order as the (4×4)-element system with conventional SM. Moreover, as also observed in Fig. 3, when increasing D, the gains saturate for higher values, which can also be seen here, where the BER for $D = 20$ closely approximates the one for $D = 100$.

In Fig. 6 the BER versus SNR performance is shown for the (4×2), (8×2), and (8×4) systems for both SM and SM-CR.

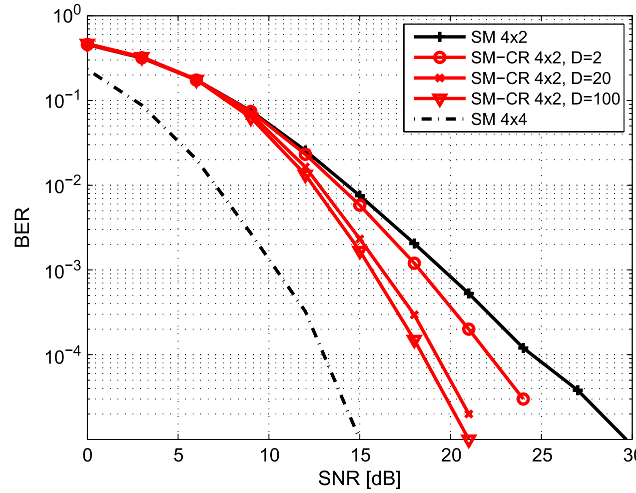

Fig. 5. BER versus SNR for a (4×2) MIMO with SM and SM-CR with $D = 2$, $D = 20$, and $D = 100$ for 4QAM.

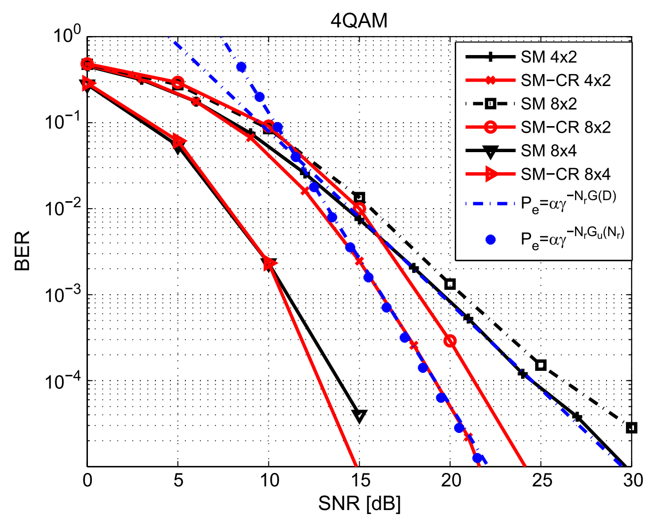

Fig. 6. BER versus SNR for a (4×2), (8×2), and (8×4) MIMO with SM and SM-CR with $D = 20$ for 4QAM.

The theoretical diversity trends observed in the form of $P_e = \alpha\gamma^{-\delta}$ are also shown, where P_e denotes the probability of error for high SNR; γ is the SNR; and $\delta = N_r G$ is the diversity order, where G is taken from the respective points in Fig. 3, which is upper bounded, as calculated in Section IV. The performance trends for both the exact diversity gains $G(D)$ based on simulation in Fig. 3 and the upper bounds $G_u(N_r)$ of Theorem 1 in Section IV-A are shown for comparison. A close match between the analytical and simulated diversity can be observed. With regard to the performance observed, it can be seen that there is indeed a performance penalty when increasing the number of TAs from four to eight for SM with fixed RA number, due to the growth of the spatial constellation, which harms the detection of the TA index [see (4×2) to (8×2)]. The improved received diversity in the detection of TA index when increasing the number of RA brings the performance benefits observed in Fig. 6 between (8×2) and (8×4). The same comparison is shown in Fig. 7 for the case of 16QAM, and it can be seen

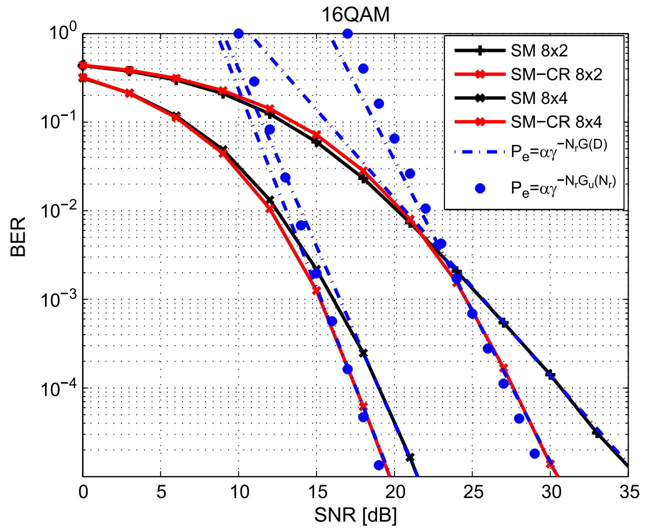

Fig. 7. BER versus SNR for a (8×2) and (8×4) MIMO with SM and SM-CR with $D = 20$ for 16QAM.

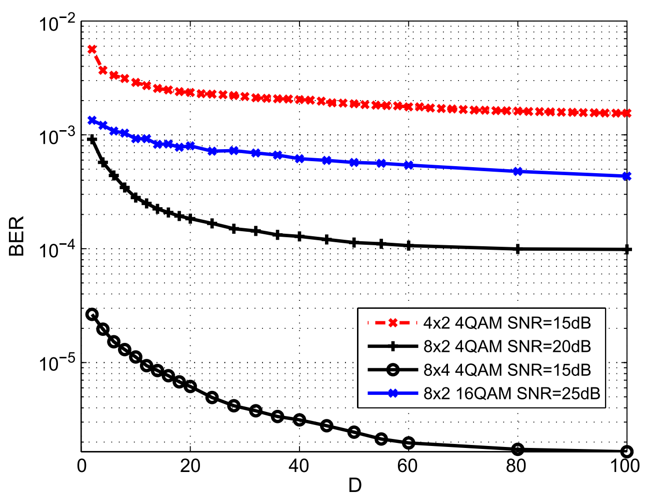

Fig. 8. BER versus D for a (4×2), (8×2), and (8×4) MIMO with SM-CR for 4QAM and 16QAM.

that the performance benefits of the proposed persist. Again, the performance trends for both the exact diversity gains $G(D)$ based on simulation in Fig. 3 and the upper bounds $G_u(N_r)$ of Theorem 1 in Section IV-A are shown for comparison. It can be observed that simulation closely matches the theoretical performance trend with both exact diversity gains and their upper bounds, verifying the increase in transmit diversity order, as proven theoretically.

Fig. 8 shows the BER as a function of D for the (4×2), (8×2), and (8×4) with 4QAM and 16QAM and various transmit SNR values. Clear gains in the BER can be observed by increasing D in its lower region, while the performance benefits saturate with increasing D in its higher region. Overall, the results illustrate how the theoretically proven gains in transmit diversity translate to improvement in the error performance for the proposed SM-CR.

The fact that the scaling factors for the proposed scheme are computed independently at the transmitter and receiver justifies

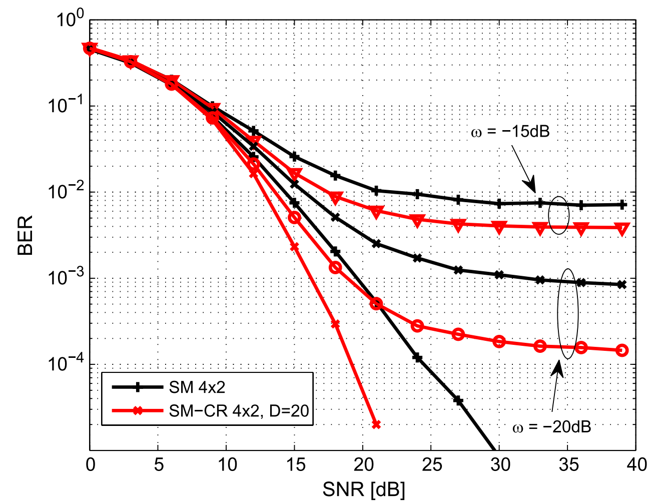

Fig. 9. BER versus SNR for a (4×2) MIMO with CSI errors for SM and SM-CR with $D = 20$, for 4QAM.

a study of the performance attainable in the presence of CSI errors and, in particular, in the case where the CSI estimated at the transmitter (CSIT) and the receiver (CSIR) are different. For this reason, in Fig. 9, we explore the situation where both the transmitter (TPS selection) and the receiver (TPS selection and ML detection) rely on erroneous CSI. We model CSIT and CSIR in the form [9]

$$\hat{\mathbf{H}} = \mathbf{H} + \mathbf{E} \tag{37}$$

where $\hat{\mathbf{H}}$ and $\mathbf{E} \sim \mathcal{CN}(0, \omega)$ are the estimated channel and the complex Gaussian CSI error having a variance ω, respectively. Independent CSI error matrices are generated at the transmitter and receiver. Fig. 9 illustrates the BER performance upon increasing the CSIT and CSIR errors for SM and SM-CR, with ω at 15 dB and 20 dB below the signal power. Both techniques are affected by the CSIR errors at the ML detection stage. In addition, for SM-CR, the errors may lead to the selection of different TPS factors at the transmitter and receiver. Nonetheless, it can be seen that both SM and SM-CR experience the same performance degradation trend with increasing the CSI errors and that the performance gains observed for SM-CR persist.

The computational complexity of the proposed technique is examined in Fig. 10, as a function of both N_t and D, for 4QAM and 16QAM. The complexity count is based on the operations calculated in Table I, and it can be seen that, for both 4QAM and 16QAM, the performance benefits of SM-CR are achieved at an increased complexity compared to SM, which scales with the selection of the parameter D. The overall tradeoff between performance and complexity is shown to be favorable for SM-CR in Fig. 11, where the power efficiency is shown with varying transit power for the (4×2) and (8×2) systems with $D = 20$. Ranges between 30 dBm (1 W) and 36 dBm (4 W) are depicted, which correspond to the power budgets of small-cell base stations [37]. It can be seen that the improved throughput for SM-CR compensates for the increased complexity in the overall system's power efficiency, thus providing an improved tradeoff compared to SM.

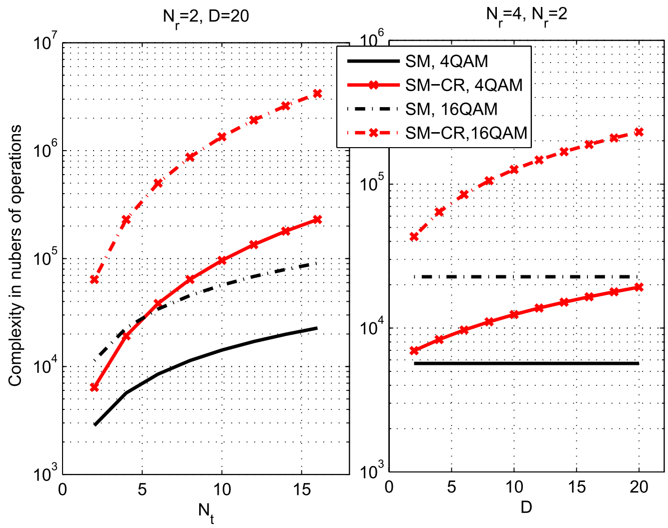

Fig. 10. Computational complexity as a function of N_t and D for SM and SM-CR for 4QAM and 16QAM.

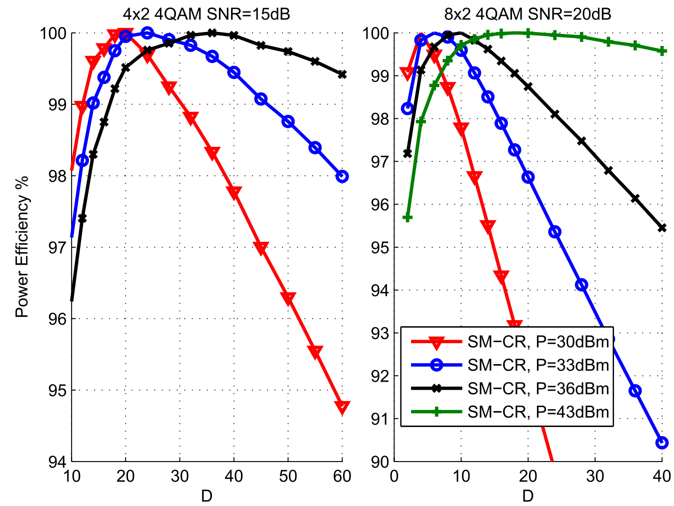

Fig. 12. Power efficiency versus D for a (4×2), (8×2) MIMO with SM and SM-CR for 4QAM.

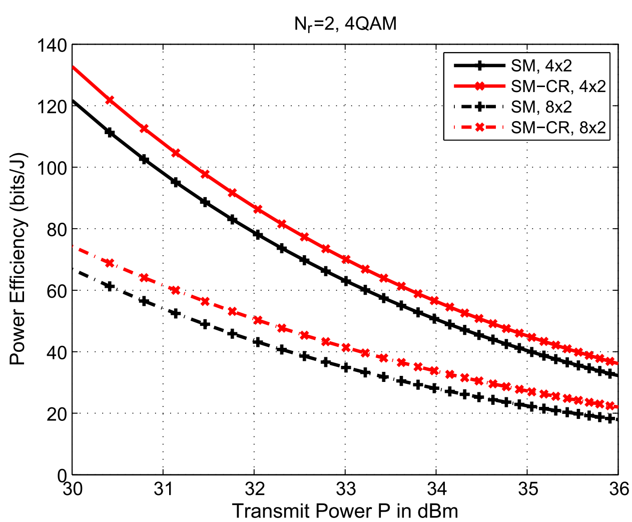

Fig. 11. Power efficiency versus P for a (4×2) and (8×2) MIMO with SM and SM-CR with $D = 20$ and $\gamma = 18$ dB for 4QAM.

Finally, Fig. 12 shows the power efficiency for increasing D for the (4×2) MIMO with transmit SNR $\gamma = 15$ dB and the (8×2) MIMO with $\gamma = 20$ dB using 4QAM modulation. The different curves in the figure represent different transmit power budgets ranging from $P = 30$ dBm to $P = 43$ dBm. For ease of illustration, power efficiency is shown as a percentage of its maximum, as the different scenarios in the figure have different maximum power efficiencies. It can be seen in both subfigures that, as the transmit power is increased, higher values of D offer the best power efficiency. This is due to the fact that, with the increase in the transmit power, the power consumption of the DSP becomes less important and the increase in throughput greatly improves the overall power efficiency. In all cases, the maximum power efficiency achieved with SM-CR is better than the one for conventional SM, which corresponds to the points in the figure with $D = 1$, indicating that the proposed scheme offers the required transmission rates at a lower power consumption.

VIII. Conclusion

A new receive-constellation-shaping approach has been introduced for SM in the MIMO channel. Conventional constellation-shaping techniques offer limited gains for SM, due to the strict fitting to a fixed constellation, and tend to require the inversion of ill-conditioned channel coefficients. Moreover, existing practical low-complexity constellation-shaping schemes are only applicable to the case where the receiver has a single antenna. We have proposed a CR scheme, where transmit diversity is introduced by appropriately selecting the TPS factors from sets of randomly generated coefficients. The proposed scheme has been shown, both analytically and by simulation, to offer significant performance gains with respect to conventional SM. Our future work will involve the application of the proposed approach to more advanced SM techniques, such as generalized SM, as well as SM with antenna selection and adaptive modulation.

References

[1] D. Gesbert, M. Kountouris, R. Heath, C.-B. Chae, and T. Salzer, "Shifting the MIMO paradigm," *IEEE Signal Process. Mag.*, vol. 24, no. 5, pp. 36–46, Sep. 2007.

[2] R. Mesleh, H. Haas, S. Sinanovic, C. W. Ahn, and S. Yun, "Spatial modulation," *IEEE Trans. Veh. Technol.*, vol. 57, no. 4, pp. 2228–2241, Jul. 2008.

[3] M. Di Renzo and H. Haas, "Bit error probability of space modulation over Nakagami-m fading: Asymptotic analysis," *IEEE Commun. Lett.*, vol. 15, no. 10, pp. 1026–1028, Oct. 2011.

[4] J. Jeganathan, A. Ghrayeb, and L. Szczecinski, "Spatial modulation: Optimal detection and performance analysis," *IEEE Commun. Lett.*, vol. 12, no. 8, pp. 545–547, Aug. 2008.

[5] A. Garcia and C. Masouros, "Low-complexity compressive sensing detection for spatial modulation in large-scale multiple access channels," *IEEE Trans. Commun.*, vol. 63, no. 7, pp. 2565–2579, Jul. 2015.

[6] A. Younis, S. Sinanovic, M. Di Renzo, R. Mesleh, and H. Haas, "Generalised sphere decoding for spatial modulation," *IEEE Trans. Commun.*, vol. 61, no. 7, pp. 2805–2815, Jul. 2013.

[7] M. Di Renzo and H. Haas, "On transmit diversity for spatial modulation MIMO: Impact of spatial constellation diagram and shaping filters at the transmitter," *IEEE Trans. Veh. Technol.*, vol. 62, no. 6, pp. 2507–2531, Jul. 2013.

[8] P. Yang *et al.*, "Star-QAM signaling constellations for spatial modulation," *IEEE Trans. Veh. Technol.*, vol. 63, no. 8, pp. 3741–3749, Oct. 2014.

[9] S. Sugiura, C. Xu, S. X. Ng, and L. Hanzo, "Coherent and differential space-time shift keying: A dispersion matrix approach," *IEEE Trans. Commun.*, vol. 59, no. 11, pp. 3090–3101, Nov. 2011.

[10] K. Ntontin, M. Di Renzo, A. Perez-Neira, and C. Verikoukis, "Adaptive generalized space shift keying," *EURASIP J. Wireless Commun. Netw.*, vol. 2013, pp. 1–15, Feb. 2013.
[11] C. Masouros and L. Hanzo, "Dual layered downlink MIMO transmission for increased bandwidth efficiency," *IEEE Trans. Veh. Technol.*, to be published.
[12] C. Masouros and L. Hanzo, "Constructive interference as an information carrier by dual layered MIMO transmission," *IEEE Trans. Veh. Technol.*, DOI: 10.1109/TVT.2015.2438776, to be published.
[13] S. Sugiura and L. Hanzo, "On the joint optimization of dispersion matrices and constellations for near-capacity irregular precoded space-time shift keying," *IEEE Trans. Wireless Commun.*, vol. 12, no. 1, pp. 380–387, Jan. 2013.
[14] Y. Xiao, Q. Tang, L. Gong, P. Yang, and Z. Yang, "Power scaling for spatial modulation with limited feedback," *Int. J. Antennas Propag.*, vol. 2013, 2013, Art. ID 718482.
[15] M. Maleki, H. Bahrami, S. Beygi, M. Kafashan, and N. H. Tran, "Space modulation with CSI: Constellation design and performance evaluation," *IEEE Trans. Veh. Technol.*, vol. 62, no. 4, pp. 1623–1634, May 2013.
[16] A. Garcia, C. Masouros, and L. Hanzo, "Pre-scaling optimization for space shift keying based on semidefinite relaxation," *IEEE Trans. Commun.*, vol. 63, no. 11, pp. 4231–4243, Nov. 2015
[17] X. Guan, Y. Cai, and W. Yang, "On the mutual information and precoding for spatial modulation with finite alphabet," *IEEE Wireless Commun. Lett.*, vol. 2, no. 4, pp. 383–386, Aug. 2013.
[18] J. M. Luna-Rivera, D. U. Campos-Delgado, and M. G. Gonzalez-Perez, "Constellation design for spatial modulation," *Procedia Technol.*, vol. 7, pp. 71–78, 2013.
[19] C. Masouros, "Improving the diversity of spatial modulation in MISO channels by phase alignment," *IEEE Commun. Lett.*, vol. 18, no. 5, pp. 729–732, May 2014.
[20] P. Yang, M. Di Renzo, Y. Xiao, S. Li, and L. Hanzo, "Design guidelines for spatial modulation," *IEEE Commun. Surveys Tuts.*, vol. 17, no. 1, pp. 6–26, 1st Quart. 2015.
[21] M. Di Renzo, H. Haas, A. Ghrayeb, S. Sugiura, and L. Hanzo, "Spatial modulation for generalized MIMO: Challenges, opportunities, and implementation," *Proc. IEEE*, vol. 102, no. 1, pp. 56–103, Jan. 2014.
[22] M. Di Renzo, H. Haas, and P. M. Grant, "Spatial modulation for multiple-antenna wireless systems: A survey," *IEEE Commun. Mag.*, vol. 49, no. 12, pp. 182–191, Dec. 2011.
[23] J. Jeganathan, A. Ghrayeb, L. Szczecinski, and A. Ceron, "Space shift keying modulation for MIMO channels," *IEEE Trans. Wireless Commun.*, vol. 8, no. 7, pp. 3692–3703, Jul. 2009.
[24] M. Di Renzo and H. Haas, "Bit error probability of SM-MIMO over generalized fading channels," *IEEE Trans. Veh. Technol.*, vol. 61, no. 3, pp. 1124–1144, Mar. 2012.
[25] M. Abramowitz and I. A. Stegun, *Handbook of Mathematical Functions With Formulas, Graphs, and Mathematical Tables*. New York, NY, USA: Dover, 1972.
[26] R. Ware and F. Lad, "Approximating the distribution for sums of products of normal variables," Univ. Canterbury, Christchurch, New Zealand, Res. Rep., 2003.
[27] H. A. David and H. N. Nagaraja, *Order Statistics*, 3rd ed. New York, NY, USA: Wiley, 2003.
[28] *Evolved Universal Terrestrial Radio Access (E-UTRA); LTE Physical Layer; General Description*, 3GPP TS 36.201, V11.1.0, Rel. 11, Mar. 2008.
[29] X. Cong, G. Y. Li, Z. Shunqing, Y. Chen, and S. Xu, "Energy- and spectral-efficiency tradeoff in downlink OFDMA networks," *IEEE Trans. Wireless Commun.*, vol. 10, no. 11, pp. 3874–3886, Nov. 2011.
[30] A. Stavridis, S. Sinanovic, M. Di Renzo, and H. Haas, "Energy evaluation of spatial modulation at a multi-antenna base station," in *Proc. IEEE 78th VTC—Fall*, Sep. 2–5, 2013, pp. 1–5.
[31] A. Stavridis, S. Sinanovic, M. Di Renzo, H. Haas, and P. Grant, "An energy saving base station employing spatial modulation," in *Proc. IEEE 17th Int. Workshop CAMAD*, Sep. 17–19, 2012, pp. 231–235.
[32] S. Cui, A. J. Goldsmith, and A. Bahai, "Energy-constrained modulation optimization," *IEEE Trans. Wireless Commun.*, vol. 4, no. 5, pp. 2349–2360, Sep. 2005.
[33] C. Masouros, M. Sellathurai, and T. Ratnarajah, "Computationally efficient vector perturbation precoding using thresholded optimization," *IEEE Trans. Commun.*, vol. 61, no. 5, pp. 1880–1890, May 2013.
[34] C. Masouros, M. Sellathurai, and T. Ratnarajah, "Maximizing energy-efficiency in the vector precoded MU-MISO downlink by selective perturbation," *IEEE Trans. Wireless Commun.*, vol. 13, no. 9, pp. 4974–4984, Sep. 2014.
[35] C. Masouros, M. Sellathurai, and T. Ratnarajah, "Vector perturbation based on symbol scaling for limited feedback MISO downlinks," *IEEE Trans. Signal Process.*, vol. 62, no. 3, pp. 562–571, Feb. 1, 2014.
[36] D. Curd, "Power consumption in 65 nm FPGAs," Xilinx, San Jose, CA, USA, White Paper, Feb. 2007.
[37] "W-CDMA open access small cells: Architecture, requirements and dependencies," Small Cell Forum Ltd, Dursley, U.K., White Paper, May 2012.

Christos Masouros (M'06–SM'14) received the Diploma in electrical and computer engineering from the University of Patras, Patras, Greece, in 2004 and the M.Sc. degree (by research) and the Ph.D. degree in electrical and electronic engineering from The University of Manchester, Manchester, U.K., in 2006 and 2009, respectively.

He is currently a Lecturer with the Department of Electrical and Electronic Engineering, University College London, London, U.K. He was previously a Research Associate with The University of Manchester and a Research Fellow with the Queen's University Belfast, Belfast, U.K. His research interests lie in the field of wireless communications and signal processing, with particular focus on green communications, large-scale antenna systems, cognitive radio, and interference mitigation techniques for multiple-input–multiple-output and multicarrier communications.

Dr. Masouros holds a Royal Academy of Engineering Research Fellowship for 2011–2016 and is the Principal Investigator of the Engineering and Physical Sciences Research Council's Project EP/M014150/1 on large-scale antenna systems. He is an Associate Editor for the IEEE COMMUNICATIONS LETTERS.

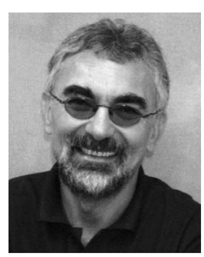

Lajos Hanzo (M'91–SM'92–F'04) received the M.S. degree in electronics and the Ph.D. degree from Budapest University of Technology and Economics (formerly, Technical University of Budapest), Budapest, Hungary, in 1976 and 1983, respectively; the D.Sc. degree from the University of Southampton, Southampton, U.K., in 2004; and the "Doctor Honoris Causa" degree from Budapest University of Technology and Economics in 2009.

During his 38-year career in telecommunications, he has held various research and academic posts in Hungary, Germany, and the U.K. Since 1986, he has been with the School of Electronics and Computer Science, University of Southampton, where he holds the Chair in Telecommunications. He is currently directing a 100-strong academic research team, working on a range of research projects in the field of wireless multimedia communications sponsored by industry, the Engineering and Physical Sciences Research Council of U.K., the European Research Council's Advanced Fellow Grant, and the Royal Society Wolfson Research Merit Award. During 2008–2012, he was a Chaired Professor with Tsinghua University, Beijing, China. He is an enthusiastic supporter of industrial and academic liaison and offers a range of industrial courses. He has successfully supervised more than 80 Ph.D. students, coauthored 20 John Wiley/IEEE Press books on mobile radio communications totaling in excess of 10 000 pages, and published more than 1400 research entries on IEEE Xplore. He has more than 20 000 citations. His research is funded by the European Research Council's Senior Research Fellow Grant.

Dr. Hanzo is a Governor of the IEEE Vehicular Technology Society. He has served as the Technical Program Committee Chair and the General Chair of IEEE conferences, has presented keynote lectures, and has been awarded a number of distinctions. During 2008–2012, he was the Editor-in-Chief of the IEEE Press. He is a Fellow of the Royal Academy of Engineering, The Institution of Engineering and Technology, and the European Association for Signal Processing.

AUTHOR QUERIES

AUTHOR PLEASE ANSWER ALL QUERIES

AQ1 = Please check if the current affiliation of author "Christos Masouros" is properly captured, to be consistent with the biography provided; otherwise, kindly provide the correction.
AQ2 = Please check if Fig. 4 is properly cited here, to properly sequence the citations; otherwise, kindly provide the correction.
AQ3 = Please check if "a factor of" here is properly captured, to make the statement clear; otherwise, kindly provide the correction.
AQ4 = Please check if the expanded form of "FPGA" is properly captured; otherwise, kindly provide the correction.
AQ5 = Please provide publication update in Ref. [12].

END OF ALL QUERIES

Constellation Randomization Achieves Transmit Diversity for Single-RF Spatial Modulation

Christos Masouros, *Senior Member, IEEE*, and Lajos Hanzo, *Fellow, IEEE*

***Abstract*—The performance of spatial modulation (SM) is known to be dominated by the minimum Euclidean distance (MED) in the received SM constellation. In this paper, a symbol-scaling technique is proposed for SM in the multiple-input–multiple-output (MIMO) channel that enhances the MED to improve the performance of SM. This is achieved by forming fixed sets of candidate prescaling factors for the transmit antennas (TAs), which are randomly generated and are known at both the transmitter and the receiver. For a given channel realization, the transmitter chooses the specific set of factors that maximizes the MED. Given the channel state information (CSI) readily available at the receiver for detection, the receiver independently chooses the same set of prescaling factors and uses them for the detection of both the antenna index (AI) and the symbol of interest. We analytically calculate the attainable gains of the proposed technique, in terms of its transmit diversity order, based on both the distribution of the MED and on the theory of classical order statistics. Furthermore, we show that the proposed scheme offers a scalable performance–complexity tradeoff for SM by varying the number of candidate sets of prescaling factors, with significant performance improvements, compared to conventional SM.**

***Index Terms*—Constellation shaping, multiple-input single-output, prescaling, spatial modulation (SM).**

I. Introduction

TRADITIONAL spatial multiplexing has been shown to improve the capacity of the wireless channel by exploiting multiantenna transmitters [1]. More recently, spatial modulation (SM) has been explored as a means of implicitly encoding information in the index of the specific antenna activated for the transmission of the modulated symbols, offering a low-complexity alternative [2]. Its central benefits include the absence of interantenna interference (IAI) and the fact that it only requires a subset (down to one) of radio-frequency (RF) chains compared to spatial multiplexing. Accordingly, the interantenna synchronization is also relaxed. Early work has focused on the design of receiver algorithms for minimizing the bit error rate (BER) of SM at a low complexity [2]–[6]. Matched filtering is shown to be a low-complexity technique for detecting the antenna index (AI) used for SM [2]. A maximum-likelihood (ML) detector is introduced in [4] for reducing the complexity of classic spatial multiplexing ML detectors. Compressive sensing and reduced-space sphere detection have been discussed for SM in [5] and [6] for further complexity reduction.

In addition to receive processing, recent work has also proposed constellation shaping for SM [7]–[15]. Specifically, in [7], the transmit diversity of coded SM is analyzed for different *spatial constellations*, which represent the legitimate sets of activated transmit antennas (TAs). Furthermore, Yang [8] discusses symbol constellation optimization for minimizing the BER. Indeed, spatial- and symbol-constellation shaping are discussed separately, as aforementioned. By contrast, the design of the received SM constellation that combines the choice of the TA, as well as the transmit symbol constellation, is the focus of this paper. Precoding-aided approaches that combine SM with spatial multiplexing are studied in [11] and [12]. A number of constellation-shaping schemes [9]–[15] have also been proposed for the special case of SM, which is referred to as space shift keying, where the information is only carried in the spatial domain, by the activated AI. Their application to the SM transmission, where the transmit waveform is modulated, is nontrivial.

Closely related work has focused on shaping the receive SM constellation by means of symbol prescaling at the transmitter, aiming at maximizing the minimum Euclidean distance (MED) in the received SM constellation [17]–[19]. The constellation-shaping approach in [17] and [18] aims at fitting the receive SM constellation to one of the existing optimal constellation formats in terms of minimum distance, such as, e.g., quadrature amplitude modulation (QAM). Due to the strict constellation fitting requirement imposed on both the amplitude and the phase, this prescaling relies on the inversion of the channel coefficients. In the case of ill-conditioned channels, this substantially increases the power associated to the transmit constellation and therefore requires scaling factors for normalizing the transmit power, which, however, reduces the received signal-to-noise ratio (SNR). This problem has been alleviated in [19], where a constellation-shaping scheme based on phase-only scaling is proposed. Nevertheless, the constellation shaping used in the aforementioned schemes is limited in the sense that it only applies to multiple-input–single-output (MISO) systems where a single symbol is received for each transmission, and thus, the characterization and shaping of the receive SM constellation is simple. The application of constellation shaping in the multiple-input–multiple-output (MIMO) systems is still an open problem.

Manuscript received September 30, 2014; revised June 3, 2015 and November 10, 2015; accepted December 27, 2015. This work was supported by the Royal Academy of Engineering, U.K. The review of this paper was coordinated by Prof. Y. Gong.

C. Masouros is with the Department of Electrical and Electronic Engineering, University College London, London WC1E 7JE, U.K. (e-mail: c.masouros@ucl.ac.uk).

AQ1

L. Hanzo is with the School of Electronics and Computer Science, University of Southampton, Southampton SO17 1BJ, U.K. (e-mail: lh@ecs.soton.ac.uk).

Color versions of one or more of the figures in this paper are available online at http://ieeexplore.ieee.org.

Digital Object Identifier 10.1109/TVT.2015.2513380

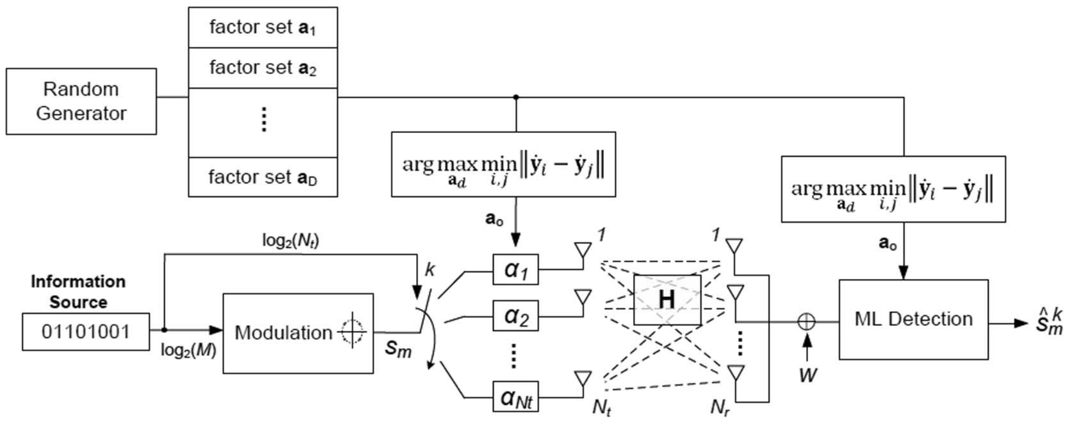

Fig. 1. Block diagram of SM transceiver with constellation randomization (SM-CR).

In line with the aforementioned challenges, in this paper, we introduce a new transmit prescaling (TPS) scheme, where the received constellation fitting problem is relaxed. As opposed to the aforementioned strict constellation fitting approaches, here, the received SM constellation is randomized by TPS for maximizing the MED between its points for a given channel. In more detail, a number of randomly generated candidate sets of TPS factors are formed offline, which are known to both the transmitter and the receiver. Each of these sets is normalized, so that the average transmit power remains unchanged, and yields a different receive constellation for a certain channel realization. For a given channel, the transmitter then selects that particular set of TPS factors that yields the SM constellation having the maximum MED. By doing so, the TPS alleviates the cases where different TAs yield similar received symbols and thus improves the reliability of symbol detection. At the receiver, by exploiting the channel state information (CSI) readily available for detection, the detector selects the same set of TPS factors to form the received constellation and applies an ML test to estimate the data. The explicit benefit of the aforementioned methodology is that it extends the idea of receive SM constellation shaping to the MIMO scenarios having multiple antennas at the receiver, and it will be shown that it introduces additional transmit diversity gains and improves the power efficiency of the SM system. Against this background, we list the main contributions of this paper as follows.

- We propose a new per-antenna TPS scheme for SM-aided point-to-point MIMO transmission that improves the attainable performance.
- We analytically derive a tight upper bound of the transmit diversity gains obtained by the proposed technique, based on the distribution of the MED in the received constellation for transmission over a frequency-flat Rayleigh distributed channel.
- We analyze the computational complexity of the proposed scheme to demonstrate how a scalable performance–complexity tradeoff can be provided by the proposed technique, when adapting the number of candidate sets of TPS factors.
- Using the aforementioned performance and complexity analyses, we study the power efficiency of the proposed scheme in comparison to conventional SM. We introduce a power efficiency metric that combines the transmit power, the achieved throughput, and the computational complexity imposed to quantify the improved power efficiency offered by the proposed scheme.

The remainder of this paper is organized as follows. Section II presents the MIMO system model and introduces the SM transmission. Section III details the proposed TPS scheme, while in Section IV, we present our analytical study of the obtained transmit diversity gains of the proposed scheme. Sections V and VI detail the complexity calculation and the study of the attainable power efficiency. Section VII presents our numerical results, and finally, our conclusions are offered in Section VIII.

II. System Model and Spatial Modulation

A. System Model

Consider a MIMO system where the transmitter and receiver are equipped with N_t and N_r antennas, respectively. For simplicity, unless stated otherwise, in this paper, we assume that the transmit power budget is limited to unity, i.e., $P = 1$. See [20]–[22] for extensive reviews and tutorials on the basics and state-of-the-art on SM. Here, we focus on the single-RF-chain SM approach, where the transmit vector is in the all-but-one zero form $\mathbf{s}_m^k = [0, \ldots, s_m, \ldots, 0]^T$, where the notation $[.]^T$ denotes the transpose operator. Here, $s_m, m \in \{1, \ldots, M\}$ is a symbol taken from an M-order modulation alphabet that represents the transmitted waveform in the baseband domain conveying $\log_2(M)$ bits, and k represents the index of the activated TA (the index of the nonzero element in $\mathbf{s}_m^k$) conveying $\log_2(N_t)$ bits in the spatial domain. Clearly, since $\mathbf{s}$ is an all-zero vector apart from s_m^k, there is no IAI.

The per-antenna TPS approach, which is the focus of this paper, is shown in Fig. 1. The signal fed to each TA is scaled by a complex-valued coefficient $\alpha_k, k \in \{1, \ldots, N_t\}$, for which we have $E\{|\alpha_k|\} = 1$, where $|x|$ denotes the amplitude of a complex number x, and $E\{.\}$ denotes the expectation operator. Defining the MIMO channel vector as $\mathbf{H}$, with elements $h_{i,j}$ representing the complex channel coefficient between the ith TA to the jth receive antenna (RA), the received symbol vector can be written as

$$\mathbf{y} = \mathbf{H}\mathbf{A}\mathbf{s}_m^k + \mathbf{w} \tag{1}$$

where $\mathbf{w} \sim \mathcal{CN}(0, \sigma^2 \mathbf{I})$ is the additive white Gaussian noise component at the receiver, with $\mathcal{CN}(\mu, \sigma^2)$ denoting the circularly symmetric complex Gaussian distribution with mean μ and variance σ^2. Furthermore, $\mathbf{A} = \mathrm{diag}(\mathbf{a}) \in \mathbb{C}^{N_t \times N_t}$ is the TPS matrix with $\mathbf{a} = [\alpha_1, \alpha_2, \ldots, \alpha_{N_t}]$, and $\mathrm{diag}(\mathbf{x})$ represents the diagonal matrix with its diagonal elements taken from vector $\mathbf{x}$. Note that the diagonal structure of $\mathbf{A}$ guarantees having a transmit vector $\mathbf{t} = \mathbf{As}$ with a single nonzero element, so that the single-RF-chain aspect of SM is preserved.

At the receiver, a joint ML detection of both the TA index and the transmit symbol is obtained by the minimization

$$\begin{aligned} [\hat{s}_m, \hat{k}] &= \arg\min_{i} \|\mathbf{y} - \mathbf{y}_i\| \\ &= \arg\min_{m,k} \left\|\mathbf{y} - \mathbf{H}\mathbf{A}\mathbf{s}_m^k\right\| \end{aligned} \tag{2}$$

where $\|\mathbf{x}\|$ denotes the norm of vector $\mathbf{x}$, and $\mathbf{y}_i$ is the ith constellation point in the received SM constellation. By exploiting the specific structure of the transmit vector, this can be further simplified to

$$[\hat{s}_m, \hat{k}] = \arg\min_{m,k} \left\|\mathbf{y} - \mathbf{h}_k \alpha_m^k s_m\right\| \tag{3}$$

where $\mathbf{h}_k$ denotes the kth column of matrix $\mathbf{H}$, and α_m^k is the TPS coefficient of the kth TA. It is widely recognized that the performance of the detection, as explained earlier, is dominated by the MED between adjacent constellation points $\dot{\mathbf{y}}_i, \dot{\mathbf{y}}_j$ in the receive SM constellation, i.e.,

$$d_{\min} = \min_{i,j} \|\mathbf{y}_i - \mathbf{y}_j\|^2, i \neq j. \tag{4}$$

Accordingly, to improve the likelihood of correct detection, constellation-shaping TPS schemes for SM aim at maximizing this MED. The optimum TPS matrix $\mathbf{A}^*$ can be found by solving the optimization

$$\begin{aligned} \mathbf{A}^* &= \arg\max_{\mathbf{A}} \min_{i,j} \|\mathbf{y}_i - \mathbf{y}_j\|^2, i \neq j \\ \text{s.t.c.} \quad & \mathrm{trace}(\mathbf{A}^{*H}\mathbf{A}^*) \leq P \end{aligned} \tag{5}$$

and, additionally for single-RF-chain SM, subject to $\mathbf{A}^*$ having a diagonal structure. As aforementioned, $\mathbf{A}^H$ and $\mathrm{trace}(\mathbf{A})$ represent the Hermitian transpose and trace of matrix $\mathbf{A}$, respectively. The aforementioned optimization, however, is an NP-hard problem, which makes finding the TPS factors prohibitively complex and motivates the conception of lower complexity suboptimal techniques.

B. *Prescaling for the MISO Channel*

In line with the aforementioned discussions, in [17], a prescaling scheme is proposed for the MISO channel. Assuming a channel vector $\mathbf{h}$, the receive SM constellation is fitted to a Q-QAM constellation with $Q = N_t M$ by choosing

$$\tilde{\alpha}_m^k = \frac{q_{(m-1)M+k}\|\mathbf{h}\|}{h_k s_m \sqrt{N_t}} \tag{6}$$

where q_i is the ith constellation point in the Q-QAM constellation, and the factor $\|\mathbf{h}\|/\sqrt{N_t}$ is used for normalizing the receive constellation so that $E\{|q|\} = 1$.

We note that, while the scaling in (6) normalizes the receive constellation, it does not normalize the transmit power. Therefore, power-normalized scaling coefficients should be used in the form

$$\alpha_m^k = \frac{\tilde{\alpha}_m^k}{\|\tilde{\mathbf{a}}\|}. \tag{7}$$

Nevertheless, it can be seen that for ill-conditioned channel coefficients, even for just one of the TAs, this leads to low power-scaling factors $f = 1/\|\tilde{\mathbf{a}}\|$, which limits the obtainable performance. Finally, note that α_m^k are data dependent for this approach, as evidenced by the index m, which does not allow for a fixed per-antenna scaling coefficient, as shown in Fig. 1. Most importantly, the aforementioned strict constellation fitting cannot be extended to systems having multiple RAs, since the inversion of the full channel matrix $\mathbf{H}$ would result in nonzero elements in the transmit vector $\mathbf{t}$, which means that all TAs are used. Therefore, the important benefit of single-RF transmission of SM is lost.

An alternative is shown in [19], again for the MISO channel, where the scaling factors are in the form

$$\alpha_k = e^{j\varphi_k} \tag{8}$$

$$\varphi_k = \theta_i - \vartheta_k \tag{9}$$

where ϑ_k is the phase of the kth channel, and θ_i is the ith angle taken from an equally spaced angle arrangement within $[0, 2\pi)$ in the form

$$\theta_i = \frac{2\pi}{N_t M}(i-1), i \in \{1, \ldots, N_t\}. \tag{10}$$

In this way, the phases of the points in the receive SM constellation become equispaced, hence maintaining a minimum for the Euclidean distances in the constellation.

Aside from their individual limitations and the fact that they are suboptimal, the aforementioned prescaling methods are limited by the fact that they apply solely to MISO systems relying on a single RA and cannot be readily extended to the case of MIMO SM transmission, hence lacking receive diversity.

III. Proposed Constellation Randomization Prescaling (SM-CR)

To alleviate the drawbacks of the aforementioned techniques, we propose an adaptive TPS technique that randomizes the received SM constellation. The proposed constellation randomization (CR) simply selects the "best" from a number of randomly generated sets of per-antenna TPS factors, with the aim of improving the resulting MED. By allowing the randomization of the amplitude and phase of the effective channel that combines the TPS factor and the channel gains of the TA, the proposed scheme relaxes the constellation optimization problem and facilitates a better solution for the maximization of $d_{\min}$. In addition, through the aforementioned randomization and selection of the appropriate TPS factors, the proposed scheme critically improves the transmit diversity of the SM system, as will be shown analytically in the following section. The proposed scheme involves the steps as analyzed in the following.

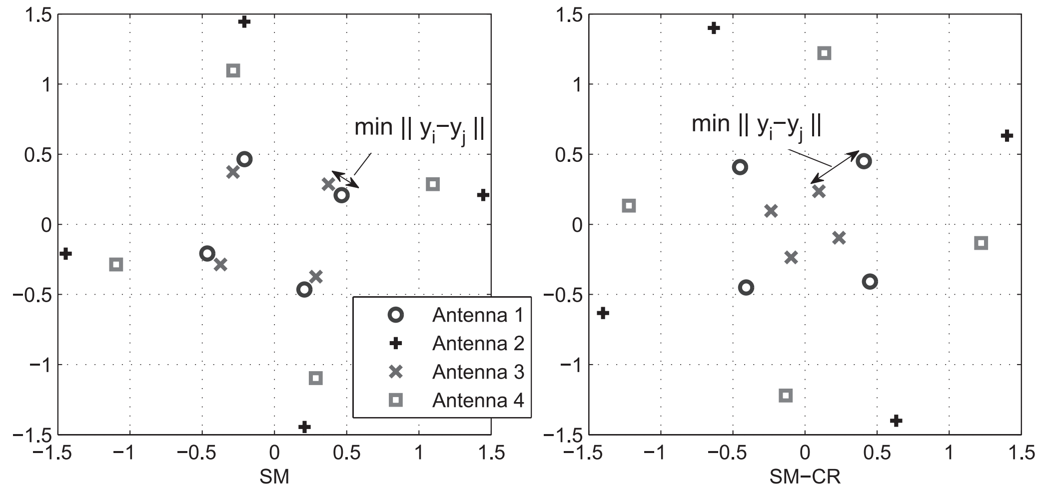

Fig. 2. Received constellation for a 4 × 1 MISO with SM and SM-CR for 4QAM.

A. Formation of Candidate Prescaling Sets

First, a number of D candidate TPS vectors are generated randomly in the form $\mathbf{a}_d$, where $d \in [1, D]$ denotes the index of the candidate set, and $\mathbf{a}_d$ is formed by the elements $\alpha_m^{k(d)} \sim \mathcal{CN}(0, 1)$. These are made available to both the transmitter and the receiver once, in an offline fashion before transmission. These assist in randomizing the received constellation, which is most useful in the cases where two points in the constellation of $\mathbf{H}\mathbf{s}_m^k, m \in [1, M], k \in [1, N_t]$ happen to be very close. To ensure that the average transmit power remains unchanged, the scaling factors are normalized as in (7). It is important to reiterate that, in this work, we focus on power-normalized scaling factors, and hence, the proposed scheme does not constitute a power-allocation scheme. This allows us to isolate the diversity gains from the power and coding gains in our analysis in the following section. In the generalized case, power allocation could be applied on top of the prescaling, by employing a diagonal power-allocation matrix, while the resulting diversity gains would not change.

B. Selection of Prescaling Vector

For a given channel, based on the knowledge of vectors $\mathbf{a}_d$, both the transmitter and the receiver can determine the received SM constellation for every d by calculating the set of $[m, k]$ possibilities in

$$\hat{\mathbf{y}} = \mathbf{H}\mathbf{A}_d\mathbf{s}_m^k \tag{11}$$

where $\mathbf{A}_d = \mathrm{diag}(\mathbf{a}_d)$ is the diagonal matrix that corresponds to the candidate set $\mathbf{a}_d$. Then, for the given channel coefficients, the transmitter and receiver can independently choose the scaling vector $\mathbf{a}_o$, for which

$$\mathbf{a}_o = \arg\max_d \min_{\substack{m_1,m_2,k_1,k_2 \\ \{m_1,k_1\}\neq\{m_2,k_2\}}} \left\|\mathbf{H}\mathbf{A}_d\mathbf{s}_{m_1}^{k_1} - \mathbf{H}\mathbf{A}_d\mathbf{s}_{m_2}^{k_2}\right\|^2. \tag{12}$$

The transmitter then sends $\mathbf{t} = \mathbf{A}_o\mathbf{s}_m^k$, with $\mathbf{A}_o = \mathrm{diag}(\mathbf{a}_o)$, and the receiver applies the ML detector according to

$$[\hat{s}_m, \hat{k}] = \arg\min_{m,k} \|\mathbf{y} - \mathbf{H}\mathbf{A}_o\mathbf{s}_m^k\|. \tag{13}$$

As mentioned earlier, since the channel coefficients are estimated at the receiver for detection [2]–[6], (12) can be used to derive the aforementioned factors independently at the receiver. Therefore, no feed forwarding of $\alpha_m^{k(d)}$ or the index d is required. Indeed, for equal channel coefficients available at the transmitter and receiver, they both select the same TPS vector $\mathbf{a}_o$ independently, as per (12). Alternatively, to dispose of the need for CSI at the transmitter (CSIT), the receiver can indeed select the best scaling factors using (12) and feed the index of the selected scaling vector $\mathbf{a}_o$ out of the D candidates back to the transmitter, using $\lceil \log_2 D \rceil$ bits. In comparison to the closely related works in [17]–[19], this provides the proposed scheme with the advantage of a reduced transmit complexity that, instead of CSIT acquisition and prescaling optimization, involves the detection of $\lceil \log_2 D \rceil$ bits at the end of every channel coherence period, and a single complex multiplication of the classically modulated symbol s_m with the prescaling factor a_m^k in the form shown in (3).

The intuitive benefits of the proposed scheme in the MED of the received SM constellation are shown in Fig. 2 for a (4 × 1)-element MISO system employing 4QAM modulation at high SNR, where the original receive SM constellation without TPS is shown in the left-hand side, and the constellation after the selection in (12) is illustrated on the right-hand side. A clear increase in the MED can be observed, without increasing the average transmit power. In fact, for the example in Fig. 2, a slight reduction of the power in the symbols denoted by "×" can be observed, which, nevertheless, increases the MED in the constellation.

Observe in Fig. 2 that while suboptimal in the constellation design sense, the proposed TPS enhances the MED in the constellation with respect to conventional SM, while imposing a conveniently scalable complexity as per the size of candidate sets D. It is evident that the gains in the MED for the proposed scheme are dependent on the set size D of the candidate TSP vector sets $\mathbf{a}_d$ to choose from. An indicative result of this dependence is shown in Fig. 3, where the average gains in the MED are shown, with increasing numbers of D for different transmission scenarios. Theoretically derived upper bounds for these gains for $N_r = 1$, $N_r = 2$, and $N_r = 4$, based

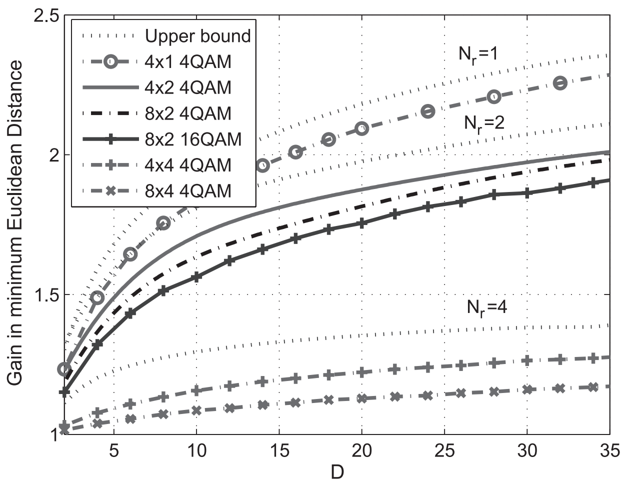

Fig. 3. Gain G in average MED for SM-CR with respect to SM for increasing D.

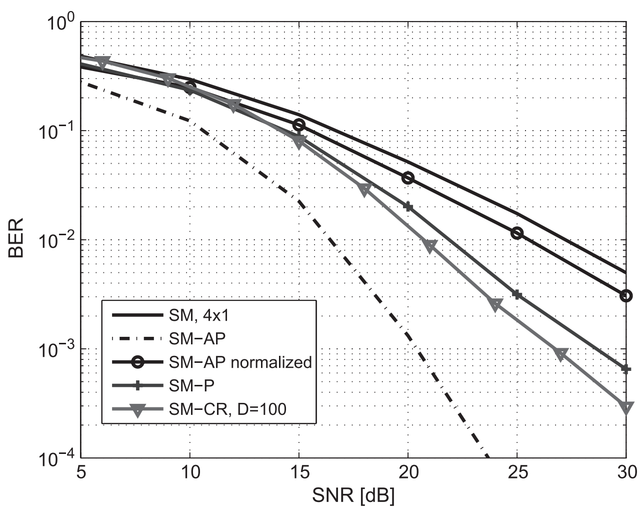

Fig. 4. BER versus SNR for a (4×1) MISO with SM, SM-AP [17], SM-P [19], and SM-CR with $D = 100$ for 4QAM.

on Theorem 1 of the following section, are also shown in the figure and will be detailed in the following. It can be seen that, for low values of D, significant MED benefits are obtained by increasing the number of candidates, while the gains saturate in the region of higher values of D. This justifies the choice of low values of D to constrain the computational complexity involved in the search in (12). In the results that follow, we explore the error rates and complexity and their tradeoff in terms of power efficiency as a means of optimizing the value of D for different performance targets.

IV. Diversity Analysis

A. Transmit Diversity

The proposed CR scheme leads to an increase in the transmit diversity gains. That is, while the transmit diversity of the single-RF SM is known to be one [7], the proposed TPS introduces an amplitude–phase diversity in the transmission, due to the existence of D candidate sets of TPS factors from which to choose. The system is said to have a diversity order of δ, if the BER decays with $\gamma^{-\delta}$ in the high-SNR region, with γ being the SNR (see Fig. 4). To analyze the attainable diversity order, we note the pairwise error probability (PEP) for SM scales with the Euclidean distance between constellation points as [7]

$$\mathrm{PEP}\,(\mathbf{y}_i, \mathbf{y}_j) = \mathcal{Q}\left(\sqrt{\frac{\|\mathbf{y}_i - \mathbf{y}_j\|^2}{2\sigma^2}}\right) \tag{14}$$

where $\mathcal{Q}(x)$ denotes the Gaussian Q-function [25], and

$$\begin{aligned}\|\mathbf{y}_i - \mathbf{y}_j\| &= \sqrt{\|\mathbf{y}_i\|^2 + \|\mathbf{y}_j\|^2 - 2\mathbf{y}_i \bullet \mathbf{y}_j} \\ &= \sqrt{\|\mathbf{y}_i\|^2 + \|\mathbf{y}_j\|^2 - 2\|\mathbf{y}_i\|\|\mathbf{y}_j\|\cos(\Delta\phi)}\end{aligned} \tag{15}$$

where $\mathbf{a} \bullet \mathbf{b}$ denotes the dot product of vectors, and $\Delta\phi$ denotes the phase difference between the two constellation points. Accordingly, for the purposes of characterizing the diversity order, we define the gain in the MED for the proposed SM-CR as

$$\begin{aligned}G(D) &\hat{=} \frac{E\{\max_d d_{\min}^d\}}{E\{d_{\min}\}} \\ &= \frac{E\{\max_d \min_{m,k} \|\mathbf{HA}_d\mathbf{s}_{m_1}^{k_1} - \mathbf{HA}_d\mathbf{s}_{m_2}^{k_2}\|^2\}}{E\{\min_{m,k} \|\mathbf{Hs}_{m_1}^{k_1} - \mathbf{Hs}_{m_2}^{k_2}\|^2\}}\end{aligned} \tag{16}$$

where we have used the notation $G(D)$ to suggest that the gain is a function of the size of candidate sets D. It will be shown in the results section that this gain also represents the transmit diversity gain attained. The following theorem describes an upper bound of this diversity gain.

Theorem 1: For a frequency-flat Rayleigh fading channel $\mathbf{H} \sim \mathcal{CN}(0, (1/2)\mathbf{I}_{N_r} \oplus \mathbf{I}_{N_t})$, the gain in the MED of the proposed SM-CR is upper bounded as

$$G(D) \leq G_u = \sum_{k=1}^{D} \binom{D}{k} (-1)^{k+1} e^{n(k-1)} \frac{Ei(-nk, nk)}{Ei(-n, n)} \tag{17}$$

where $n \hat{=} \binom{N_t M}{2}$, with $\binom{p}{q} = p!/q!(p-q)!$ denoting the binomial coefficient, with $x!$ being the factorial function and $Ei(-n, n)$ denoting the generalized exponential integral function [25].

Proof: To simplify the analysis, we shall assume that the distances in the receive constellation are statistically independent. It is shown in Fig. 2 that, strictly speaking, this is not true since the constellation points created by each channel are indeed interdependent through the transmit symbol constellation. Nevertheless, we will demonstrate in Fig. 3 that this affordable assumption yields a tight upper bound for the gain. First, regarding the product $\mathbf{HA}_d$, it has been shown in [26] that the product of uncorrelated zero-mean Gaussian variables with variances σ_1^2, σ_2^2 is also zero-mean Gaussian with a variance equal to $\sigma_{\Pi}^2 = \sigma_1^2\sigma_2^2$. It is therefore clear that, for a normalized transmit constellation, the receive vectors are distributed as $\mathbf{y}_i \sim \mathcal{CN}(0, 1/2\mathbf{I}_{N_r})$. Accordingly, $\mathbf{y}_i - \mathbf{y}_j \sim \mathcal{CN}(0, \mathbf{I}_{N_r})$, and therefore, $z \hat{=} \|\mathbf{y}_i - \mathbf{y}_j\|^2 \sim \mathcal{X}_{2N_r}^2$, where $\mathcal{X}_k^2$ denotes the chi-square distribution with k degrees of freedom [25]. The probability density function (PDF) and cumulative distribution function (CDF) of z are, therefore, given by

$$f_z(x) = \frac{1}{2^{N_r}\Gamma(N_r)} x^{N_r - 1} e^{-x/2} \tag{18}$$

$$F_z(x) = \frac{1}{\Gamma(N_r)} \gamma\left(N_r, \frac{x}{2}\right) \tag{19}$$

where $\Gamma(.)$ and $\gamma(.,.)$ denote the Gamma and lower incomplete Gamma functions, respectively [25]. Based on the theory of order statistics [27], from the $n \hat{=} \binom{N_t M}{2}$ distances in the receive SM constellation (see Fig. 2), the minimum distance is distributed as

$$\begin{aligned} f_{d_{\min}}(x) &= n f_z(x)[1-F_z(x)]^{n-1} \\ &= \frac{n}{2^{N_r}\Gamma(N_r)^n} x^{N_r-1} e^{-x/2} \left[\Gamma\left(N_r, \frac{x}{2}\right)\right]^{n-1} \quad (20) \\ F_{d_{\min}}(x) &= 1-(1-F_z(x))^n \\ &= 1-\left[\frac{1}{\Gamma(N_r)}\Gamma\left(N_r, \frac{x}{2}\right)\right]^n \quad (21) \end{aligned}$$

where $\Gamma(.,.)$ denotes the upper incomplete Gamma function and, as mentioned earlier, it is assumed that all distances in the receive SM constellation are independent. Since $d_{\min}$ is nonnegative, its mean is found as

$$\begin{aligned} E\{d_{\min}\} &= \int_0^\infty [1-F_{d_{\min}}(x)]dx \\ &= \int_0^\infty [1-F_z(x)]^n dx. \quad (22) \end{aligned}$$

Let us now derive the mean of the maximum minimum distance in the receive SM constellation as per the proposed technique. We note that, for the normalized TPS factors in (7), the distribution of $\mathbf{y}_i$ remains unchanged. Therefore, the PDF and CDF of $\tau \hat{=} \max_{\mathbf{A}_d} d_{\min}$, when selecting the maximum from D, candidates are given as

$$f_\tau(x) = D f_{d_{\min}}(x) F_{d_{\min}}(x)^{D-1} \quad (23)$$

$$F_\tau(x) = F_{d_{\min}}(x)^D. \quad (24)$$

Similarly to the aforementioned calculation, for the mean of $\tau \hat{=} \max_{\mathbf{A}_d} d_{\min}$, we have

$$\begin{aligned} E\{\tau\} &= \int_0^\infty \{1-F_\tau(x)\}\, dx \\ &= \int_0^\infty \left\{1-F_{d_{\min}}(x)^D\right\} dx \\ &= \int_0^\infty \left\{1-[1-(1-F_z(x))^n]^D\right\} dx \\ &= \int_0^\infty \left\{1-\sum_{k=0}^{D}\binom{D}{k}(-1)^k(1-F_z(x))^{nk}\right\} dx \\ &= \sum_{k=1}^{D}\binom{D}{k}(-1)^{k+1}\int_0^\infty (1-F_z(x))^{nk}dx. \quad (25) \end{aligned}$$

As stated previously, we have used the binomial expansion $(1-x)^m = \sum_{k=0}^m \binom{m}{k}(-1)^k x^k$. By substituting (22) and (25) into (16), we arrive at the upper bound for the gain in the MED as

$$G_u(N_r) = \sum_{k=1}^{D}\binom{D}{k}(-1)^{k+1}\frac{\int_0^\infty (1-F_z(x))^{nk}dx}{\int_0^\infty (1-F_z(x))^n dx} \quad (26)$$

where we have used the notation $G_u(N_r)$ to clarify that the upper bound here is a function of N_r. Finally, it can be shown that $(dG_u(N_r)/dN_r) \leq 0$, and therefore, the gain is a monotonically decreasing function of the number of RAs. Hence, the gain for the case $N_r = 1$ provides a global upper bound for all cases of N_r. Indeed, as it is shown in Fig. 3 and is intuitive, the highest gains can be observed for the single-antenna receiver case, which experiences a diversity of one for conventional SM. For this case, from (18), (19), and (26), we get (17). ■

B. Error Probability Trends

Based on the aforementioned diversity calculations, we can derive the BER performance of the proposed scheme in the high-SNR region. Indeed, SM systems with N_r uncorrelated RAs have been shown to experience a unit transmit diversity order and receive diversity order of N_r. Accordingly, since the proposed scheme attains a transmit diversity order of $G(D)$, the total diversity becomes $\delta = N_r G(D)$. The resulting probability of error P_e follows the trend

$$P_e = \alpha \gamma^{-N_r G(D)} \quad (27)$$

where γ is the transmit SNR, $\delta = N_r G(D)$ is the diversity order based on the calculations of $G(D)$ in Section IV-A, and α is an arbitrary coefficient. The diversity order $\delta = N_r G(D)$ accounts for the inherent receive diversity N_r in the system and the transmit diversity $G(D)$ induced by the proposed scheme. Clearly, as per the upper bound of Theorem 1 in (17) and the P_e trend in (27), a lower bound in the resulting probability of error can be obtained. In the following results, we show that the aforementioned performance trend matches the simulated performance in the high-SNR region.

V. Computational Complexity

It is clear from the aforementioned discussion that the proposed SM-CR leads to an increase in the computational complexity, with respect to conventional SM, due to the need to compute the MED for all the D candidate scaling factor sets. Here, we analyze the increase in computational complexity at the receiver. We later use this analysis to model the power consumption associated with the required signal processing and compare the proposed SM-CR with conventional SM, in terms of the overall power efficiency of transmission. For reference, we have assumed an LTE Type 2 TDD frame structure [28]. This has a 10-ms duration, which consists of 10 subframes, out of which five subframes, containing 14 symbol time slots each, are used for downlink transmission yielding a block size of $B = 70$ for the downlink, while the rest are used for both uplink and control information transmission. A slow-fading channel is assumed, where the channel remains constant for the duration of the frame. In Table I, we summarize the computationally dominant operations involved at the receiver for both SM and SM-CR. In these calculations, we have used the fact that the calculation of the norm of a vector with n elements involves $2n$ elementary operations. In addition, it can be seen that the product $\mathbf{A}_d \mathbf{s}_m^k$ is a scalar that involves a single complex-valued multiplication, and its multiplication with the channel matrix involves an additional $2N_r$ elementary operations per

TABLE I
COMPLEXITY FOR SM AND THE PROPOSED SM-CR SCHEME

SM-CR		Operations	SM		Operations
Constellation Optimization			*Constellation Calculation*		
$\mathbf{HA}_d\mathbf{s}_m^k, \forall m, k$	$\times D$	$(2N_r+1)N_tMD$	$\mathbf{Hs}_m^k, \forall m, k$		$(2N_r+1)N_tM$
$\mathbf{f}_{m_1,m_2}^{k_1,k_2(d)} = \|\|\mathbf{HA}_d\mathbf{s}_{m_1}^{k_1} - \mathbf{HA}_d\mathbf{s}_{m_2}^{k_2}\|\|$, $\forall m_1, m_2, k_1, k_2, m_1 \neq m_2, k_1 \neq k_2$	$\times D$	$2N_r\binom{N_tM}{2}D$			
$d_{min}^{(d)} = \min\{\mathbf{f}_{m_1,m_2}^{k_1,k_2(d)}\}$	$\times D$	$\binom{N_tM}{2}D$			
$\mathbf{A}_o = \arg\max d_{min}^{(d)}$		D			
ML Detection					
$g_m^k = \|\|\mathbf{y} - \mathbf{HA}_o\mathbf{s}_m^k\|\|^2, \forall m, k$	$\times B$	$2N_tMN_rB$	$g_m^k = \|\|\mathbf{y} - \mathbf{Hs}_m^k\|\|^2, \forall m, k$	$\times B$	$2N_tMN_rB$
$\arg\min g_m^k$	$\times B$	N_tMB	$\arg\min g_m^k$	$\times B$	N_tMB
Total: $(2Nr+1)\left[\binom{N_tM}{2} + N_tM\right]D + D + (2N_r+1)N_tMB$			Total: $(2N_r+1)N_tM(B+1)$		

constellation point. This has to be done for each of the N_tM points in the receive constellation. Accordingly, there are a number of $\binom{N_tM}{2}$ distances in the constellation, and therefore, there are $\binom{N_tM}{2}$ norms in the form of (12) that need to be calculated for each candidate scaling factor set. The first three operations in the constellation optimization in Table I need to be done for each candidate set: hence, D times in total. For the ML detection, a number of N_tM norms in the form of (13) need to be calculated before the minimum is chosen, and this has to be calculated B times in the frame. Finally, we have used the fact that finding the maximum and the minimum in an n-element vector requires n operations.

Based on the aforementioned calculations, we have the complexities of the SM receiver and of the SM-CR receiver, respectively, in the form of

$$C_{\rm SM}(D) = (2N_r+1)N_tM(B+1) \tag{28}$$

$$C_{\rm SM-CR}(D) = (2Nr+1)\left[\binom{N_tM}{2} + N_tM\right]D + D + (2Nr+1)N_tMB \tag{29}$$

where it can be seen that the complexity of SM-CR is in the form

$$C_{\rm SM-CR}(D) = \chi D + \psi \tag{30}$$

with

$$\chi = (2Nr+1)\left[\binom{N_tM}{2} + N_tM\right] + 1 \tag{31}$$

$$\psi = (2Nr+1)N_tMB. \tag{32}$$

In the following section, we use these expressions to calculate the resulting power consumption related to signal processing at the receiver for the evaluation of the power efficiency of transmission.

VI. POWER EFFICIENCY

As the ultimate metric for evaluating the performance–complexity tradeoff and the overall usefulness of the proposed technique, and toward an energy-efficient communication system, we consider the power efficiency of SM-CR compared to SM, as well as its dependence on the number of candidate scaling factor sets D. We note that prior studies explore the energy efficiency of SM for the purposes of optimizing the number of antennas employed [30], [31]. Following the modeling in [29] and [32]–[35], we define the transmit power efficiency of the communication link as the bit rate per total transmit power dissipated, i.e., the ratio of the throughput achieved over the consumed power as

$$\mathcal{P} = \frac{T}{P_{\rm PA} + (1+N_r)\cdot P_{\rm RF} + p_c \cdot C} \tag{33}$$

where $P_{\rm PA} = ((\xi/\eta) - 1)P$ in watts is the power consumed at the power amplifier to produce the total transmit signal power P, with η being the power amplifier efficiency and ξ being the modulation-dependent peak-to-average power ratio. Furthermore, $P_{\rm RF} = P_{\rm mix} + P_{\rm filt} + P_{\rm DAC}$ is the power related to the mixers, to the transmit filters, and to the digital-to-analog converter (DAC), which is assumed constant for the purposes of this work. We use practical values of these from [32] as $\eta = 0.35$ and $P_{\rm mix} = 30.3$ mW, $P_{\rm filt} = 2.5$ mW, and $P_{\rm DAC} = 1.6$ mW, yielding $P_{\rm RF} = 34.4$ mW. In (33), p_c in watts/Kops is the power per 10^3 elementary operations (KOps) of the digital signal processor (DSP), and C is the number of operations involved. This term is used to introduce complexity as a factor of the transmitter power consumption in the power efficiency metric. Typical values of p_c include $p_c = 22.88$ mW/KOps for the Virtex-4 and $p_c = 5.76$ mW/KOps for the Virtex-5 field-programmable gate array family from Xilinx [36]. Finally

$$T = \mathcal{E}B(1-P_B) = \mathcal{E}B(1-P_e)^B \tag{34}$$

represents the achieved throughput, where P_B is the block error rate, and

$$\mathcal{E} = \log_2(N_tM) \tag{35}$$

is the spectral efficiency of SM in bits per channel use. For a given transmit power and numbers of TAs and RAs, combining (33) with (27), the power efficiency expression for SM-CR takes the form

$$\mathcal{P} = \frac{\mathcal{E}B(1-\alpha\gamma^{-N_rG(D)})^B}{c + p_cC(D)} \tag{36}$$

where both $G(D)$ and $C(D)$ are functions of the number of candidate sets D through (26) and (29), while α, c are constants. This expression can therefore be used to characterize the scalable performance–complexity tradeoff for the proposed scheme and for optimizing the value of D for maximizing power efficiency.

The expression in (33) provides an amalgamated metric that combines throughput, complexity, and transmit signal power, all in a unified metric. By varying the number of candidate scaling factor sets D, both the resulting complexity and transmission rates are influenced, as shown earlier. Therefore, a scalable tradeoff between performance and complexity can be achieved accordingly. High values of $\mathcal{P}$ indicate that high bit rates are achievable for a given power consumption, and thus denote a high energy efficiency. The following results show that SM-CR provides an increased energy efficiency compared to SM in numerous scenarios using different transmit powers P.

VII. Simulation Results

To evaluate the benefits of the proposed technique, this section presents numerical results based on Monte Carlo simulations of conventional SM without scaling (termed as SM in the figures) and the proposed SM-CR. Our focus is on systems where the receiver employs more than one antenna, where the prescaling schemes in [17]–[19] are inapplicable. The channel impulse response is assumed to be perfectly known at the transmitter. Without loss of generality, unless stated otherwise, we assume that the transmit power is restricted to $P = 1$. MIMO systems with up to eight TAs employing 4QAM and 16QAM modulation are explored, albeit it is plausible that the benefits of the proposed technique extend to larger scale systems and higher order modulation.

First, for reasons of reference, the BER performance of the proposed scheme is compared with the performance of the most relevant techniques in [17] and [19] for the MISO channel, where the latter techniques are applicable. First, we note the performance loss when applying power scaling to the scheme in [17]. Second, while the true strength of the proposed lies in the fact that it applies to MIMO links where the schemes in [17] and [19] are inapplicable, the results here show that the proposed scheme outperforms the conventional techniques in the MISO channel as well.

Next, we show the BER performance with increasing transmit SNR for a (4×2)-element MIMO employing 4QAM, for various numbers of candidate scaling factor sets D, in Fig. 5. The graph includes the performance of SM for the (4×4)-element MIMO for reference. It can be seen that the slope of the BER curves increases with increasing D, which indicates an increase in transmit diversity order. Indeed, for high values of D, the (4×2)-element system with SM-CR exhibits the same transmit diversity order as the (4×4)-element system with conventional SM. Moreover, as also observed in Fig. 3, when increasing D, the gains saturate for higher values, which can also be seen here, where the BER for $D = 20$ closely approximates the one for $D = 100$.

In Fig. 6 the BER versus SNR performance is shown for the (4×2), (8×2), and (8×4) systems for both SM and SM-CR.

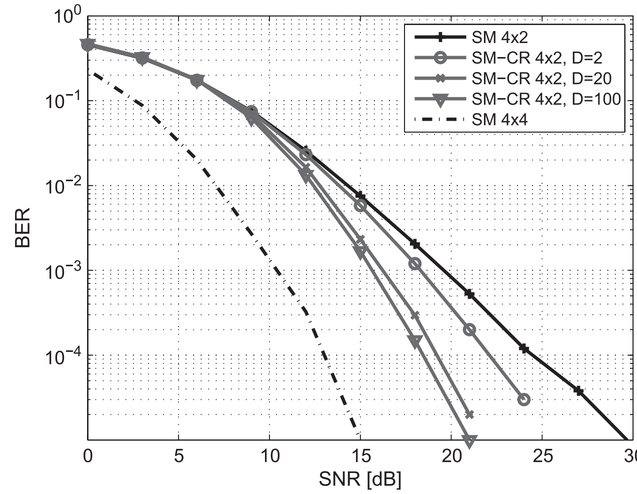

Fig. 5. BER versus SNR for a (4×2) MIMO with SM and SM-CR with $D = 2$, $D = 20$, and $D = 100$ for 4QAM.

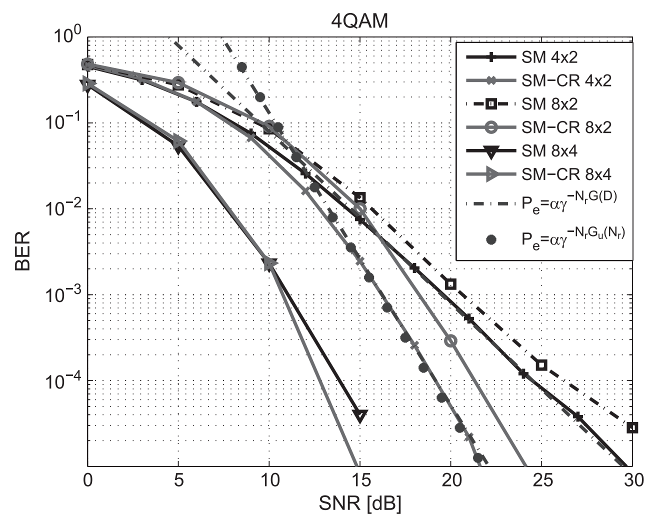

Fig. 6. BER versus SNR for a (4×2), (8×2), and (8×4) MIMO with SM and SM-CR with $D = 20$ for 4QAM.

The theoretical diversity trends observed in the form of $P_e = \alpha\gamma^{-\delta}$ are also shown, where P_e denotes the probability of error for high SNR; γ is the SNR; and $\delta = N_r G$ is the diversity order, where G is taken from the respective points in Fig. 3, which is upper bounded, as calculated in Section IV. The performance trends for both the exact diversity gains $G(D)$ based on simulation in Fig. 3 and the upper bounds $G_u(N_r)$ of Theorem 1 in Section IV-A are shown for comparison. A close match between the analytical and simulated diversity can be observed. With regard to the performance observed, it can be seen that there is indeed a performance penalty when increasing the number of TAs from four to eight for SM with fixed RA number, due to the growth of the spatial constellation, which harms the detection of the TA index [see (4×2) to (8×2)]. The improved received diversity in the detection of TA index when increasing the number of RA brings the performance benefits observed in Fig. 6 between (8×2) and (8×4). The same comparison is shown in Fig. 7 for the case of 16QAM, and it can be seen

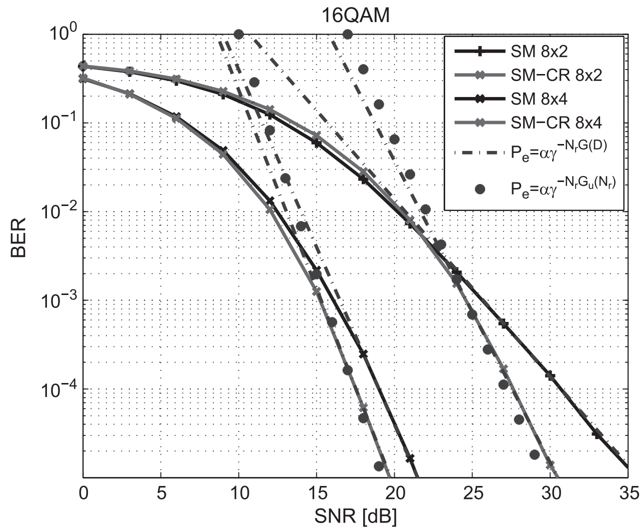

Fig. 7. BER versus SNR for a (8 × 2) and (8 × 4) MIMO with SM and SM-CR with $D = 20$ for 16QAM.

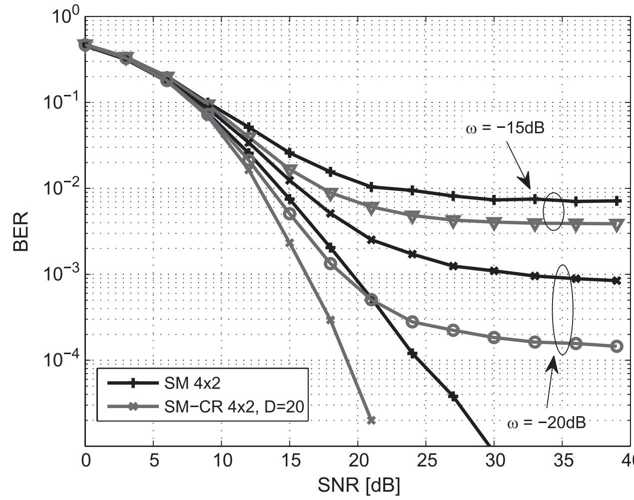

Fig. 9. BER versus SNR for a (4 × 2) MIMO with CSI errors for SM and SM-CR with $D = 20$, for 4QAM.

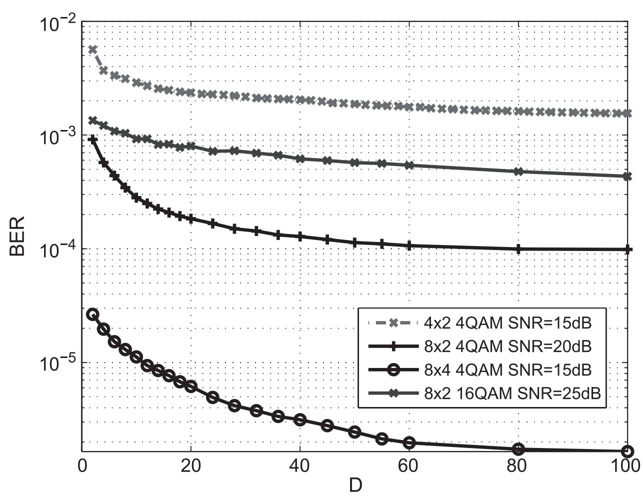

Fig. 8. BER versus D for a (4 × 2), (8 × 2), and (8 × 4) MIMO with SM-CR for 4QAM and 16QAM.

that the performance benefits of the proposed persist. Again, the performance trends for both the exact diversity gains $G(D)$ based on simulation in Fig. 3 and the upper bounds $G_u(N_r)$ of Theorem 1 in Section IV-A are shown for comparison. It can be observed that simulation closely matches the theoretical performance trend with both exact diversity gains and their upper bounds, verifying the increase in transmit diversity order, as proven theoretically.

Fig. 8 shows the BER as a function of D for the (4 × 2), (8 × 2), and (8 × 4) with 4QAM and 16QAM and various transmit SNR values. Clear gains in the BER can be observed by increasing D in its lower region, while the performance benefits saturate with increasing D in its higher region. Overall, the results illustrate how the theoretically proven gains in transmit diversity translate to improvement in the error performance for the proposed SM-CR.

The fact that the scaling factors for the proposed scheme are computed independently at the transmitter and receiver justifies a study of the performance attainable in the presence of CSI errors and, in particular, in the case where the CSI estimated at the transmitter (CSIT) and the receiver (CSIR) are different. For this reason, in Fig. 9, we explore the situation where both the transmitter (TPS selection) and the receiver (TPS selection and ML detection) rely on erroneous CSI. We model CSIT and CSIR in the form [9]

$$\hat{\mathbf{H}} = \mathbf{H} + \mathbf{E} \tag{37}$$

where $\hat{\mathbf{H}}$ and $\mathbf{E} \sim \mathcal{CN}(0, \omega)$ are the estimated channel and the complex Gaussian CSI error having a variance ω, respectively. Independent CSI error matrices are generated at the transmitter and receiver. Fig. 9 illustrates the BER performance upon increasing the CSIT and CSIR errors for SM and SM-CR, with ω at 15 dB and 20 dB below the signal power. Both techniques are affected by the CSIR errors at the ML detection stage. In addition, for SM-CR, the errors may lead to the selection of different TPS factors at the transmitter and receiver. Nonetheless, it can be seen that both SM and SM-CR experience the same performance degradation trend with increasing the CSI errors and that the performance gains observed for SM-CR persist.

The computational complexity of the proposed technique is examined in Fig. 10, as a function of both N_t and D, for 4QAM and 16QAM. The complexity count is based on the operations calculated in Table I, and it can be seen that, for both 4QAM and 16QAM, the performance benefits of SM-CR are achieved at an increased complexity compared to SM, which scales with the selection of the parameter D. The overall tradeoff between performance and complexity is shown to be favorable for SM-CR in Fig. 11, where the power efficiency is shown with varying transit power for the (4 × 2) and (8 × 2) systems with $D = 20$. Ranges between 30 dBm (1 W) and 36 dBm (4 W) are depicted, which correspond to the power budgets of small-cell base stations [37]. It can be seen that the improved throughput for SM-CR compensates for the increased complexity in the overall system's power efficiency, thus providing an improved tradeoff compared to SM.

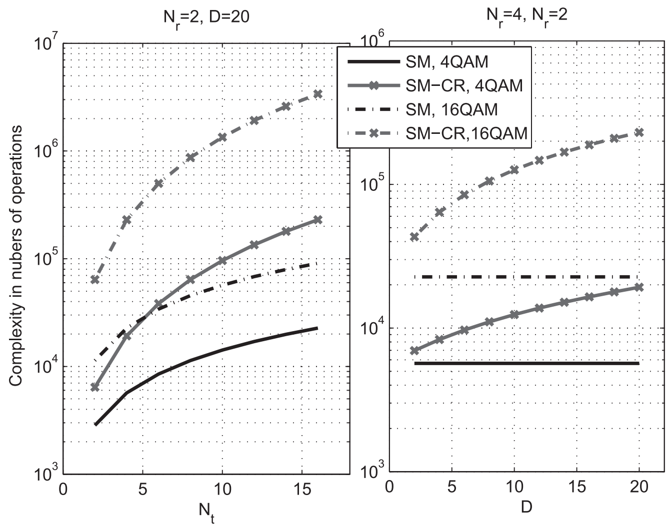

Fig. 10. Computational complexity as a function of N_t and D for SM and SM-CR for 4QAM and 16QAM.

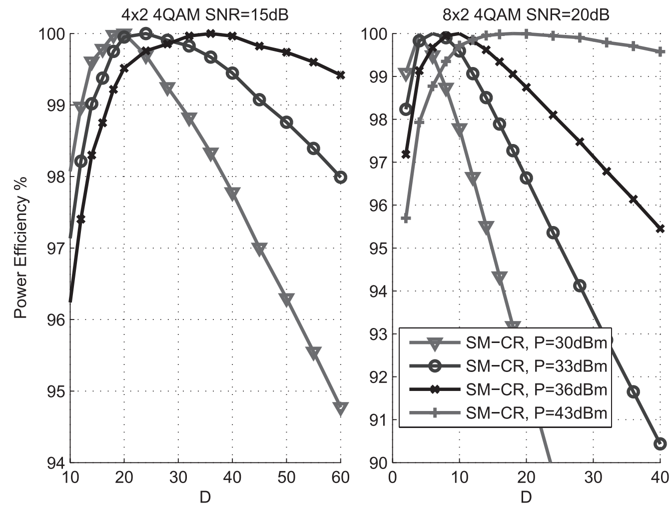

Fig. 12. Power efficiency versus D for a (4×2), (8×2) MIMO with SM and SM-CR for 4QAM.

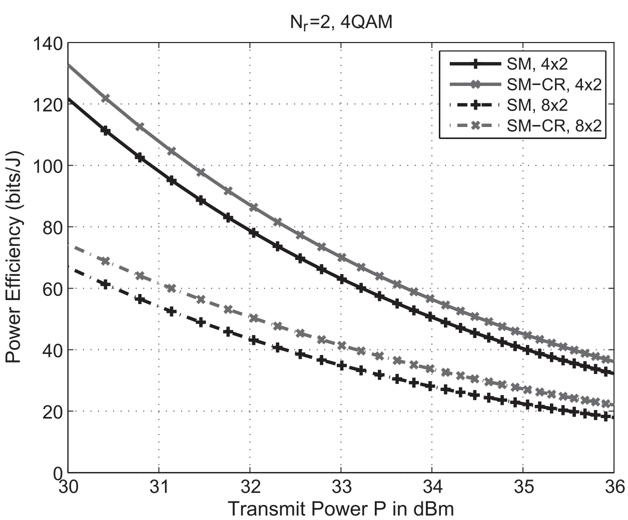

Fig. 11. Power efficiency versus P for a (4×2) and (8×2) MIMO with SM and SM-CR with $D = 20$ and $\gamma = 18$ dB for 4QAM.

Finally, Fig. 12 shows the power efficiency for increasing D for the (4×2) MIMO with transmit SNR $\gamma = 15$ dB and the (8×2) MIMO with $\gamma = 20$ dB using 4QAM modulation. The different curves in the figure represent different transmit power budgets ranging from $P = 30$ dBm to $P = 43$ dBm. For ease of illustration, power efficiency is shown as a percentage of its maximum, as the different scenarios in the figure have different maximum power efficiencies. It can be seen in both subfigures that, as the transmit power is increased, higher values of D offer the best power efficiency. This is due to the fact that, with the increase in the transmit power, the power consumption of the DSP becomes less important and the increase in throughput greatly improves the overall power efficiency. In all cases, the maximum power efficiency achieved with SM-CR is better than the one for conventional SM, which corresponds to the points in the figure with $D = 1$, indicating that the proposed scheme offers the required transmission rates at a lower power consumption.

VIII. Conclusion

A new receive-constellation-shaping approach has been introduced for SM in the MIMO channel. Conventional constellation-shaping techniques offer limited gains for SM, due to the strict fitting to a fixed constellation, and tend to require the inversion of ill-conditioned channel coefficients. Moreover, existing practical low-complexity constellation-shaping schemes are only applicable to the case where the receiver has a single antenna. We have proposed a CR scheme, where transmit diversity is introduced by appropriately selecting the TPS factors from sets of randomly generated coefficients. The proposed scheme has been shown, both analytically and by simulation, to offer significant performance gains with respect to conventional SM. Our future work will involve the application of the proposed approach to more advanced SM techniques, such as generalized SM, as well as SM with antenna selection and adaptive modulation.

References

[1] D. Gesbert, M. Kountouris, R. Heath, C.-B. Chae, and T. Salzer, "Shifting the MIMO paradigm," *IEEE Signal Process. Mag.*, vol. 24, no. 5, pp. 36–46, Sep. 2007.

[2] R. Mesleh, H. Haas, S. Sinanovic, C. W. Ahn, and S. Yun, "Spatial modulation," *IEEE Trans. Veh. Technol.*, vol. 57, no. 4, pp. 2228–2241, Jul. 2008.

[3] M. Di Renzo and H. Haas, "Bit error probability of space modulation over Nakagami-m fading: Asymptotic analysis," *IEEE Commun. Lett.*, vol. 15, no. 10, pp. 1026–1028, Oct. 2011.

[4] J. Jeganathan, A. Ghrayeb, and L. Szczecinski, "Spatial modulation: Optimal detection and performance analysis," *IEEE Commun. Lett.*, vol. 12, no. 8, pp. 545–547, Aug. 2008.

[5] A. Garcia and C. Masouros, "Low-complexity compressive sensing detection for spatial modulation in large-scale multiple access channels," *IEEE Trans. Commun.*, vol. 63, no. 7, pp. 2565–2579, Jul. 2015.

[6] A. Younis, S. Sinanovic, M. Di Renzo, R. Mesleh, and H. Haas, "Generalised sphere decoding for spatial modulation," *IEEE Trans. Commun.*, vol. 61, no. 7, pp. 2805–2815, Jul. 2013.

[7] M. Di Renzo and H. Haas, "On transmit diversity for spatial modulation MIMO: Impact of spatial constellation diagram and shaping filters at the transmitter," *IEEE Trans. Veh. Technol.*, vol. 62, no. 6, pp. 2507–2531, Jul. 2013.

[8] P. Yang *et al.*, "Star-QAM signaling constellations for spatial modulation," *IEEE Trans. Veh. Technol.*, vol. 63, no. 8, pp. 3741–3749, Oct. 2014.

[9] S. Sugiura, C. Xu, S. X. Ng, and L. Hanzo, "Coherent and differential space-time shift keying: A dispersion matrix approach," *IEEE Trans. Commun.*, vol. 59, no. 11, pp. 3090–3101, Nov. 2011.

[10] K. Ntontin, M. Di Renzo, A. Perez-Neira, and C. Verikoukis, "Adaptive generalized space shift keying," *EURASIP J. Wireless Commun. Netw.*, vol. 2013, pp. 1–15, Feb. 2013.

[11] C. Masouros and L. Hanzo, "Dual layered downlink MIMO transmission for increased bandwidth efficiency," *IEEE Trans. Veh. Technol.*, to be published.

[12] C. Masouros and L. Hanzo, "Constructive interference as an information carrier by dual layered MIMO transmission," *IEEE Trans. Veh. Technol.*, DOI: 10.1109/TVT.2015.2438776, to be published.

[13] S. Sugiura and L. Hanzo, "On the joint optimization of dispersion matrices and constellations for near-capacity irregular precoded space-time shift keying," *IEEE Trans. Wireless Commun.*, vol. 12, no. 1, pp. 380–387, Jan. 2013.

[14] Y. Xiao, Q. Tang, L. Gong, P. Yang, and Z. Yang, "Power scaling for spatial modulation with limited feedback," *Int. J. Antennas Propag.*, vol. 2013, 2013, Art. ID 718482.

[15] M. Maleki, H. Bahrami, S. Beygi, M. Kafashan, and N. H. Tran, "Space modulation with CSI: Constellation design and performance evaluation," *IEEE Trans. Veh. Technol.*, vol. 62, no. 4, pp. 1623–1634, May 2013.

[16] A. Garcia, C. Masouros, and L. Hanzo, "Pre-scaling optimization for space shift keying based on semidefinite relaxation," *IEEE Trans. Commun.*, vol. 63, no. 11, pp. 4231–4243, Nov. 2015

[17] X. Guan, Y. Cai, and W. Yang, "On the mutual information and precoding for spatial modulation with finite alphabet," *IEEE Wireless Commun. Lett.*, vol. 2, no. 4, pp. 383–386, Aug. 2013.

[18] J. M. Luna-Rivera, D. U. Campos-Delgado, and M. G. Gonzalez-Perez, "Constellation design for spatial modulation," *Procedia Technol.*, vol. 7, pp. 71–78, 2013.

[19] C. Masouros, "Improving the diversity of spatial modulation in MISO channels by phase alignment," *IEEE Commun. Lett.*, vol. 18, no. 5, pp. 729–732, May 2014.

[20] P. Yang, M. Di Renzo, Y. Xiao, S. Li, and L. Hanzo, "Design guidelines for spatial modulation," *IEEE Commun. Surveys Tuts.*, vol. 17, no. 1, pp. 6–26, 1st Quart. 2015.

[21] M. Di Renzo, H. Haas, A. Ghrayeb, S. Sugiura, and L. Hanzo, "Spatial modulation for generalized MIMO: Challenges, opportunities, and implementation," *Proc. IEEE*, vol. 102, no. 1, pp. 56–103, Jan. 2014.

[22] M. Di Renzo, H. Haas, and P. M. Grant, "Spatial modulation for multiple-antenna wireless systems: A survey," *IEEE Commun. Mag.*, vol. 49, no. 12, pp. 182–191, Dec. 2011.

[23] J. Jeganathan, A. Ghrayeb, L. Szczecinski, and A. Ceron, "Space shift keying modulation for MIMO channels," *IEEE Trans. Wireless Commun.*, vol. 8, no. 7, pp. 3692–3703, Jul. 2009.

[24] M. Di Renzo and H. Haas, "Bit error probability of SM-MIMO over generalized fading channels," *IEEE Trans. Veh. Technol.*, vol. 61, no. 3, pp. 1124–1144, Mar. 2012.

[25] M. Abramowitz and I. A. Stegun, *Handbook of Mathematical Functions With Formulas, Graphs, and Mathematical Tables*. New York, NY, USA: Dover, 1972.

[26] R. Ware and F. Lad, "Approximating the distribution for sums of products of normal variables," Univ. Canterbury, Christchurch, New Zealand, Res. Rep., 2003.

[27] H. A. David and H. N. Nagaraja, *Order Statistics*, 3rd ed. New York, NY, USA: Wiley, 2003.

[28] *Evolved Universal Terrestrial Radio Access (E-UTRA); LTE Physical Layer; General Description*, 3GPP TS 36.201, V11.1.0, Rel. 11, Mar. 2008.

[29] X. Cong, G. Y. Li, Z. Shunqing, Y. Chen, and S. Xu, "Energy- and spectral-efficiency tradeoff in downlink OFDMA networks," *IEEE Trans. Wireless Commun.*, vol. 10, no. 11, pp. 3874–3886, Nov. 2011.

[30] A. Stavridis, S. Sinanovic, M. Di Renzo, and H. Haas, "Energy evaluation of spatial modulation at a multi-antenna base station," in *Proc. IEEE 78th VTC—Fall*, Sep. 2–5, 2013, pp. 1–5.

[31] A. Stavridis, S. Sinanovic, M. Di Renzo, H. Haas, and P. Grant, "An energy saving base station employing spatial modulation," in *Proc. IEEE 17th Int. Workshop CAMAD*, Sep. 17–19, 2012, pp. 231–235.

[32] S. Cui, A. J. Goldsmith, and A. Bahai, "Energy-constrained modulation optimization," *IEEE Trans. Wireless Commun.*, vol. 4, no. 5, pp. 2349–2360, Sep. 2005.

[33] C. Masouros, M. Sellathurai, and T. Ratnarajah, "Computationally efficient vector perturbation precoding using thresholded optimization," *IEEE Trans. Commun.*, vol. 61, no. 5, pp. 1880–1890, May 2013.

[34] C. Masouros, M. Sellathurai, and T. Ratnarajah, "Maximizing energy-efficiency in the vector precoded MU-MISO downlink by selective perturbation," *IEEE Trans. Wireless Commun.*, vol. 13, no. 9, pp. 4974–4984, Sep. 2014.

[35] C. Masouros, M. Sellathurai, and T. Ratnarajah, "Vector perturbation based on symbol scaling for limited feedback MISO downlinks," *IEEE Trans. Signal Process.*, vol. 62, no. 3, pp. 562–571, Feb. 1, 2014.

[36] D. Curd, "Power consumption in 65 nm FPGAs," Xilinx, San Jose, CA, USA, White Paper, Feb. 2007.

[37] "W-CDMA open access small cells: Architecture, requirements and dependencies," Small Cell Forum Ltd, Dursley, U.K., White Paper, May 2012.

Christos Masouros (M'06–SM'14) received the Diploma in electrical and computer engineering from the University of Patras, Patras, Greece, in 2004 and the M.Sc. degree (by research) and the Ph.D. degree in electrical and electronic engineering from The University of Manchester, Manchester, U.K., in 2006 and 2009, respectively.

He is currently a Lecturer with the Department of Electrical and Electronic Engineering, University College London, London, U.K. He was previously a Research Associate with The University of Manchester and a Research Fellow with the Queen's University Belfast, Belfast, U.K. His research interests lie in the field of wireless communications and signal processing, with particular focus on green communications, large-scale antenna systems, cognitive radio, and interference mitigation techniques for multiple-input–multiple-output and multicarrier communications.

Dr. Masouros holds a Royal Academy of Engineering Research Fellowship for 2011–2016 and is the Principal Investigator of the Engineering and Physical Sciences Research Council's Project EP/M014150/1 on large-scale antenna systems. He is an Associate Editor for the IEEE COMMUNICATIONS LETTERS.

Lajos Hanzo (M'91–SM'92–F'04) received the M.S. degree in electronics and the Ph.D. degree from Budapest University of Technology and Economics (formerly, Technical University of Budapest), Budapest, Hungary, in 1976 and 1983, respectively; the D.Sc. degree from the University of Southampton, Southampton, U.K., in 2004; and the "Doctor Honoris Causa" degree from Budapest University of Technology and Economics in 2009.

During his 38-year career in telecommunications, he has held various research and academic posts in Hungary, Germany, and the U.K. Since 1986, he has been with the School of Electronics and Computer Science, University of Southampton, where he holds the Chair in Telecommunications. He is currently directing a 100-strong academic research team, working on a range of research projects in the field of wireless multimedia communications sponsored by industry, the Engineering and Physical Sciences Research Council of U.K., the European Research Council's Advanced Fellow Grant, and the Royal Society Wolfson Research Merit Award. During 2008–2012, he was a Chaired Professor with Tsinghua University, Beijing, China. He is an enthusiastic supporter of industrial and academic liaison and offers a range of industrial courses. He has successfully supervised more than 80 Ph.D. students, coauthored 20 John Wiley/IEEE Press books on mobile radio communications totaling in excess of 10 000 pages, and published more than 1400 research entries on IEEE Xplore. He has more than 20 000 citations. His research is funded by the European Research Council's Senior Research Fellow Grant.

Dr. Hanzo is a Governor of the IEEE Vehicular Technology Society. He has served as the Technical Program Committee Chair and the General Chair of IEEE conferences, has presented keynote lectures, and has been awarded a number of distinctions. During 2008–2012, he was the Editor-in-Chief of the IEEE Press. He is a Fellow of the Royal Academy of Engineering, The Institution of Engineering and Technology, and the European Association for Signal Processing.

AUTHOR QUERIES

AUTHOR PLEASE ANSWER ALL QUERIES

AQ1 = Please check if the current affiliation of author "Christos Masouros" is properly captured, to be consistent with the biography provided; otherwise, kindly provide the correction.

AQ2 = Please check if Fig. 4 is properly cited here, to properly sequence the citations; otherwise, kindly provide the correction.

AQ3 = Please check if "a factor of" here is properly captured, to make the statement clear; otherwise, kindly provide the correction.

AQ4 = Please check if the expanded form of "FPGA" is properly captured; otherwise, kindly provide the correction.

AQ5 = Please provide publication update in Ref. [12].

END OF ALL QUERIES